Metallomics

Cite this: *Metallomics*, 2011, **3**, 444–463

www.rsc.org/metallomics

CRITICAL REVIEW

The "magic numbers" of metallothionein

Duncan E. K. Sutherland and Martin J. Stillman*

Received 21st December 2010, Accepted 23rd February 2011
DOI: 10.1039/c0mt00102c

Metallothioneins (MT) are a family of small cysteine rich proteins, which since their discovery in 1957, have been implicated in a range of roles including toxic metal detoxification, protection against oxidative stress, and as a metallochaperone involved in the homeostasis of both zinc and copper. The most well studied member of the family is the mammalian metallothionein, which consists of two domains: a β-domain with 9 cysteine residues, which sequesters 3 Cd^{2+} or Zn^{2+} or 6 Cu^{+} ions, and an α-domain with 11 cysteine residues and, which sequesters 4 Cd^{2+} or Zn^{2+} or 6 Cu^{+} ions. Despite over half a century of research, the exact functions of MT are still unknown. Much of current research aims to elucidate the mechanism of metal binding, as well as to isolate intermediates in metal exchange reactions; reactions necessary to maintain homeostatic equilibrium. These studies further our understanding of the role(s) of this remarkable and ubiquitous protein. Recently, supermetallated forms of the protein, where supermetallation describes metallation in excess of traditional levels, have been reported. These species may potentially be the metal exchange intermediates necessary to maintain homeostatic equilibrium. This review focuses on recent advances in the understanding of the mechanistic properties of metal binding, the implications for the metal induced protein folding reactions proposed for metallothionein metallation, the value of "magic numbers", which we informally define as the commonly determined metal-to-protein stoichiometric ratios and the significance of the new supermetallated states of the protein and the possible interpretation of the structural properties of this new metallation status. Together we provide a commentary on current experimental and theoretical advances and frame our consideration in terms of the possible functions of MT.

Department of Chemistry, The University of Western Ontario, London, ON, Canada. E-mail: martin.stillman@uwo.ca; Tel: +1 519-661-3821 ext. 83821

I. Introduction

Metallothioneins (MTs) are a group of metalloproteins characterized by their small size, high cysteine content, an absence of

Martin Stillman and Duncan Sutherland

Duncan Sutherland, from Thunder Bay, Ontario, is a PhD student with Martin Stillman. He has a B.Sc.(Hons) in Biochemistry and Chemistry from the University of Western Ontario for which he received the gold medal. He currently holds an Alexander Graham Bell Canada Graduate Scholarship awarded by NSERC of Canada. Duncan's current research interests are the mechanistics of metal binding, specifically focusing on the low affinity binding sites recently found in mammalian metallothionein using ^{113}Cd NMR and ESI-MS techniques.
Martin Stillman received his BSc and PhD from the University of East Anglia, Norwich. His PhD research focused on the application of MCD spectroscopy to porphyrins, phthalocyanines and the protein myoglobin, carried out under the supervision of Professor Andrew Thomson FRS. He was a postdoctoral fellow at the University of Alberta, Canada studying the optical properties of phthalocyanines and the enzyme horseradish peroxidase. In 1975 he moved to the University of Western Ontario, where since 1986 he has been Professor of Chemistry. He chairs the Canadian bioinorganic conference, CanBIC, held every two years in Parry Sound, Ontario. CanBIC-3 is planned for May 2011. He is a member of the organizing committee for ICBIC-15 to be held in Vancouver in August 2011. Stillman's recent publications concern the fundamental metallation reactions of metallothioneins, an understanding of the electronic structure of porphyrins and phthalocyanines, and the determination of the mechanism of heme binding in the iron scavenging proteins in the pathogenic Staphylococcus aureus bacteria.

disulfide bonds, and a lack of aromatic amino acids.[1] Metallothioneins bind strongly to the monovalent Group 11 and the divalent Group 12, d^{10} metals. The effect of binding to these soft Group 11 and 12 metals on the cysteinyl thiols is to reduce the pK_a of the cysteines by up to 6 orders of magnitude. As a consequence, the cysteine sulfurs bind to the metals as thiolates. Key to the discussion in this paper is that the formation of these metal–thiolate (cysteine) bonds dominates the secondary structure of the protein, so that we may describe the secondary and tertiary structures present in the native metallated protein as arising primarily as a result of metal-induced folding. MT was initially isolated by Margoshes and Vallee in 1957 from samples of horse kidney cortex that through progressive purification showed an increase in relative cadmium content.[2] The protein was named metallothionein for its unusually high metal and sulfur content.[3] Since its discovery, members of the MT family have been isolated from a wide array of sources including all animal phyla, fungi, plants, as well as cyanobacteria.[4] Owing to both the high cysteine content of these proteins (~30%) and their presence in all organisms, MT is implicated in a number of physiological processes. The most commonly cited processes are metal ion homeostasis, toxic metal detoxification, and protection against oxidative stress.

The most well studied member, the mammalian MTs, comprise 20 cysteine residues that act to encapsulate two metal–thiolate cores (β and α) using a combination of bridging and terminal thiolates from the cysteinyl residues (Fig. 1). The two separate domains form a dumb-bell-like structure in the crystal first described from analysis of the X-ray diffraction data from rat liver MT.[5] The β-domain with 9 cysteine residues is capable of binding 3 Cd^{2+} or Zn^{2+}, or 6 Cu^{+} and the α-domain with 11 cysteine residues capable of binding 4 Cd^{2+} or Zn^{2+}, or 6 Cu^{+}. Molecular modelling and later experimental data from solution studies suggests that the two domains are not isolated but rather somewhat coalesced. MT binds a wide range of metals with similar stoichiometries, but we may consider them not to be 'natural'. We describe these additional binding motifs below. A common thread in the mammalian MTs is, however, the formation of the two metal–thiolate clusters where a mixture of metals can bind in each domain and where the metals in either domain can be different. The question of the extent of domain interaction in the function of MTs is a current topic of intense research.

The MT family contains a number of isoforms (and subisoforms) where the complement of these is organism dependent. In particular, mammals contain four MT subfamilies that have been proposed to exhibit specific roles:[6] MT-1 and MT-2 in the liver and kidneys, which are induced by a number of stimuli including metal ions, glucocorticoids, cytokines and oxidative stress,[4,7,8] MT-3, primarily found in the central nervous system,[9] and MT-4, found in certain stratified squamous epithelial tissues.[10] While a number of stimuli can induce expression of both MT-1 and MT-2, the expression of MT-3 and MT-4 is more strictly controlled. Presumably, differences in expression are the result of both MT-3 and MT-4 having specific biological functions. To support the proposal for specificity of function, disruption of the natural expression of MT-3, through ectopic expression in mice, has been shown to cause pancreatic acinar cell necrosis and death.[11]

II. Functions

1 Metal ion homeostasis

Naturally occurring MTs are usually isolated as either Zn-MT, Cu-MT or as the mixed metal species Zn,Cu-MT and Zn,Cd-MT. In the case of mammals, Zn-MT is the dominant form,[12] however, Cu-MT has been isolated from several sources including fetal liver MT,[13,14] bovine calf liver MT,[15] rat kidney,[16] as well as brain specific MT-3.[9] Elevated Cu-MT levels have also been found in patients suffering from Wilson's disease.[17] While in the case of yeast and fungi, Cu-MT is the dominant species.[18]

At the cellular level both toxic and nontoxic metals are tightly controlled and estimates of free Cu^{+} and Zn^{2+} suggest that neither is available in the cytosol.[19,20] The absence of freely available Cu^{+} and Zn^{2+} suggests that an organism is able to exist in this state by using metallochaperones to transport these ions in a controlled manner. MT is considered one such metallochaperone, which is capable of transporting essential Zn^{2+} and Cu^{+} to apo-enzymes.[21–24] Indeed metal exchange experiments have been conducted in which Zn^{2+} from Zn_7-βα-MT has been transferred to Zn-dependent enzymes, for example, m-aconitase,[21] carbonic anhydrase,[22] and the prototypical transcription factor, Gal4.[23] Removal of Zn^{2+} from the zinc finger-containing transcription factor Sp1 demonstrates that MT may also act as a Zn^{2+} acceptor.[24] Thus this natural association of MT with the biologically essential Zn^{2+} and Cu^{+} has suggested that one of the functions of MT is the maintenance of metal ion homeostasis. While metal exchange to apo-enzymes requiring these metals has been reported, no mechanistic details have emerged yet about how the metal transfer takes place.

Support for the role of MT as a metallochaperone is found in the transcription of DNA to RNA, which has been shown to be strongly controlled by exposure to metal ions, for example in yeast,[25,26] *Drosophila*[27] and mammals.[28–30] In the case of mammals, of the four isoforms (MT-1 to -4) only two (MT-1 and MT-2) are strongly upregulated by metal ions. Induction of inducible MT isoforms requires both the interaction of a metal response element (MRE) with a metal response element binding transcription factor 1 (MTF-1). MREs are *cis*-acting DNA sequences necessary and sufficient for metallothionein expression under heavy metal load.[28,31] MTF-1 is a zinc binding protein that contains six Cys_2-His_2 zinc fingers, the presence of these zinc fingers, along with differences in their respective affinity, make MTF-1 exquisitely sensitive to changes in the concentration of zinc in a cell.[32,33] Cell free transcription experiments have shown a number of stresses, including exposure to Cd^{2+}, Cu^{+} and H_2O_2 function by displacing naturally bound Zn^{2+} from MT.[34] These free Zn^{2+} ions bind to MTF-1 leading to a translocation of MTF-1 from the cytoplasm to the nucleus where the Zn-MTF-1 interacts with MREs leading to upregulation of MT. In this way, MT is capable of countering and deactivating a wide range of insults in order to return an organism to homeostatic balance.

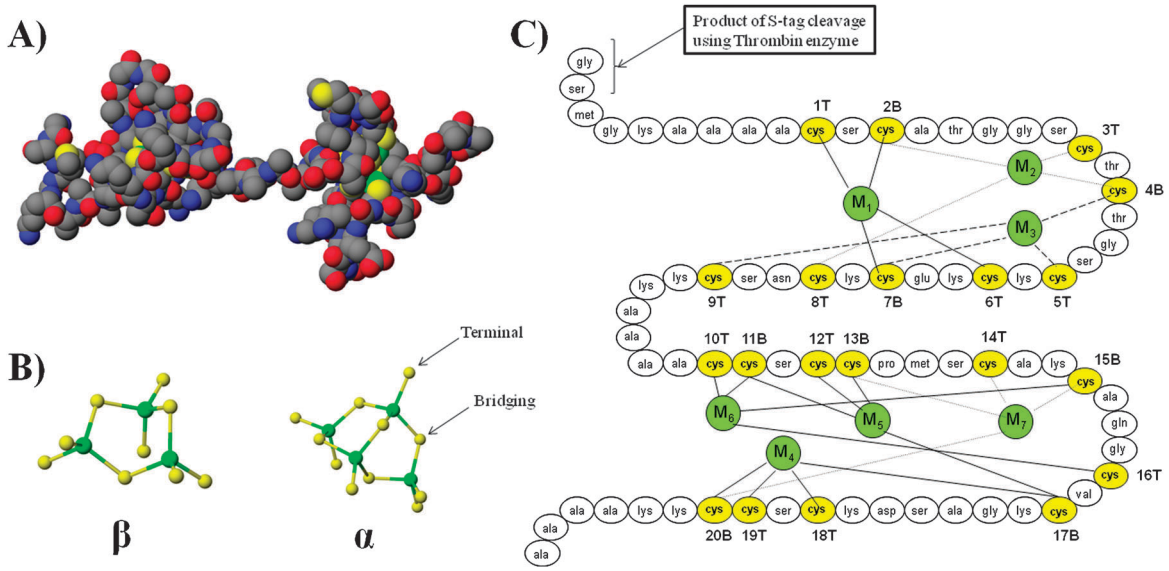

Fig. 1 (A) Space filling structure of cadmium metallated recombinant human MT-1a (Cd_7-βα-rhMT 1a) calculated using molecular modeling. The N-terminal β domain is located on the left hand side, while the C-terminal α domain is located on the right-hand side. (B) The cadmium-cysteinyl-thiolate connections, both terminal and bridging, in Cd_7-βα-rhMT 1a are presented as a ball-and-stick model: β domain (left) and α domain (right). The α domain has one bridging and one terminal thiolate labelled to clearly illustrate the different modes of coordination. (C) Connectivity diagram of human metallothionein 1a, which shows that each of the seven cadmium atoms is connected to exactly four cysteine amino acids in a tetrahedral arrangement. The cysteine residues have been numbered one through twenty and with the additional label T or B representing terminal or bridging cysteine thiolates, respectively. In the nomenclature used here, the 'recombinant' source is noted by a prefix of 'r', and the origin of the sequence is indicated by the second prefix, here 'h' for human. Molecular modeling data from Chan *et al.*[153]

2 Toxic metal detoxification

The proposed detoxifying properties of MT were inferred from metal analysis of samples isolated from human kidneys.[35,36] These samples contained significant amounts of Cd^{2+} and Hg^{2+}, the presence of Hg^{2+} being traced back to the use of therapeutic mercurial diuretics. In addition to Cd^{2+} and Hg^{2+}, MT is generally understood to coordinate all the group 11 and 12 metals, and is also capable of binding to other metals including: Co^{2+}, Pb^{2+}, $Pt^{2+/4+}$, Fe^{2+}, As^{3+}, Bi^{3+} and Tc^{5+}.[37–41] The binding affinities of MT for metal ions follows closely with the association constant of metal ions for inorganic thiolate ligands ($Hg^{2+} > Cu^{+} > Cd^{2+} > Zn^{2+}$). Thus MT preferentially coordinates many toxic metals and ultimately this coordination leads to the release of Zn^{2+}, which acts to upregulate the production of MT and returns an organism to homeostatic balance.

The requirement for and the toxicological effects of excess Zn^{2+} have been well documented.[42] MT knockout studies have highlighted the importance of this protein[43] in the homeostasis of Zn^{2+}. For example, MT-null mouse pups fed severely deficient Zn^{2+} diets, showed delays in kidney development when compared to wild-type controls. These pups lacked a hepatic reservoir of zinc critical for proper development. On the other hand, MT-null adult mice challenged with increased Zn^{2+} showed a greater incidence of pancreatic acinar cell degeneration. In this case, MT is able to act as a temporary sink to accommodate the influx of Zn^{2+}. These results demonstrate that MT is critical in protecting an organism from the extremes of Zn^{2+} exposure, acting as both a source and a sink for Zn^{2+} during deficiency and excess, respectively.

Copper toxicity is also of considerable interest, because unlike zinc, free copper is able to catalyze the formation of hydroxyl radicals through Haber-Weiss and Fenton reactions.[42] Significant regulation of copper transport in humans relies on two homologous copper transport proteins: namely, ATP7A and ATP7B.[44] Mutations to ATP7A result in Menkes disease, where copper accumulates in the kidneys and intestinal wall, while the brain, serum and liver do not receive adequate amounts.[45] A murine model of Menkes disease involving MT-1 and -2 knockout mice demonstrated that in the absence of inducible MT, knockout mice were more susceptible to copper toxicity.[46] The second disorder, Wilson's disease, resulting from mutations to ATP7B, is characterized by the accumulation of copper in the liver leading to cellular damage and release of free copper into the blood serum.[44] Cellular damage is somewhat mitigated by the accumulation of copper in the form of Cu-MT.[17,47] In this manner, MT is able to sequester Cu^{+}, and with 20 thiol groups can act as a reducing agent to further protect against oxidative stress.[48,49]

Chronic cadmium poisoning significantly affects the kidneys. Traditionally, the nephrotoxicity of Cd^{2+} exposure was thought to be the result of a transfer of Cd-MT from the liver to the kidneys with subsequent degradation leading to a high local concentration of Cd^{2+}. Indeed liver transplant studies aimed at monitoring Cd-MT levels have shown a time dependent decrease in Cd-MT present in the liver with concomitant increase of Cd-MT present in the kidneys.[50] Further complicating the problem, recent studies have demonstrated that MT knockout mice are hypersensitive to Cd^{2+}, while only accumulating 7% Cd^{2+} compared to their wild-type mice. However, it is not a paradox that MT-knockout mice only accumulate

little Cd^{2+}, but are sensitive to Cd^{2+}. Little accumulation in knockout mice would suggest that free Cd^{2+} is travelling directly to the kidneys and subsequently harming the organ. These results indicated that MT enhances the accumulation of Cd^{2+} in the kidneys but that it also significantly reduces the associated toxic effects.[51] It should be noted at this point that retention of Cd^{2+} in humans is primarily attributed to MT and that the biological half-life of Cd^{2+} in the human body is on the order of several decades.[52,53]

MT knockout mice, in which both MT-1 and MT-2 were inactivated, experience enhanced hepatic Cd^{2+} poisoning, but under control conditions these MT-null mice were viable and reproduced normally.[54] These results suggest that MT acts to buffer the toxic effects of Cd^{2+} to an organism by sequestering the Cd^{2+}, likely leading to the release of Zn^{2+}, which would act to upregulate MT. To further support the buffering role of MT, wild-type mice given increasing doses of Cd^{2+} developed a tolerance to Cd^{2+} lethality, as evidenced by a 7-fold increase in the LD_{50}.[55] While under the same conditions, the LD_{50} of MT-null mice was unaffected. These pretreatment experiments underscore the importance of not only MT in toxic metal detoxification, but also the total MT pool in an organism.

The ability of methylmercury ($MeHg^{+}$) to induce neurotoxic effects in a cell is related to the amount of MT present, with increasing amounts directly attenuating the associated toxic effects.[56] The astrocyte is thought to play a pivotal role in $MeHg^{+}$ mediated death, because it expresses three times as much MT as its associated neurons[7,8] and could potentially function as a buffer to protect these neurons, and consequently the organism, from toxic insult.[56] Surprisingly $MeHg^{+}$ is not capable of directly inducing MT in spite of its large affinity for thiol groups. We consider that MT, binding metals in a noncooperative fashion, will coordinate $MeHg^{+}$ through the available thiols found in any of the partially metallated forms.[57–59]

3 Protection against oxidative stress

The high thiol content of MT makes it an ideal molecule to interact with and inhibit reactive oxygen species (ROS). Indeed, animal studies, in which cardiac specific MT is overexpressed, have shown that MT functions to protect against oxidative stress, specifically in the inhibition of ischemia-reperfusion induced myocardial injury.[60,61] MT is upregulated by ROS through the antioxidant response element (ARE), a promoter region on the MT gene, ARE-binding transcription factors, as well as MTF-1.[48] Perhaps the most well known reactivity of MT is that with air leading to oxidation of the cysteine residues and subsequent formation of sulfoxides and disulfide bonds. Metal free (apo-) MT is particularly susceptible to oxygen, and metallation experiments should be carried out under strictly anaerobic conditions.

Nitric oxide has also been shown to increase the intracellular release of Zn^{2+} through the oxidation of Zn-MT in mouse lung fibroblasts.[62] *In vitro* analysis of the oxidation products of the three isoforms (MT -1, -2, and -3), suggests the mechanism of oxidation of each is different. In the case of mouse MT-1, the β-domain metals are exclusively released,[63] while the products from the oxidation of rabbit MT-2 show a more distributed release pattern,[64] and finally, for human MT-3 a long lived Cd_2-α-domain intermediate exists when nitric oxide induces oxidation of the protein.[65] It is probable that these differences in metal release are the result of the distinct functions of each isoform under nitrosative stress. Both cell free and cell culture studies of Zn-MT in the presence of H_2O_2 have also shown that MT is capable of acting as an antioxidant leading to release of Zn^{2+}, which acts to upregulate MT through MTF-1.[34,66,67]

Metal ions are a significant source of ROS cellular chemistry with both copper and iron capable of producing hydroxide radicals.[68] Zn-MT is capable of inhibiting the production of copper catalyzed hydroxyl radicals *in vitro*. With 20 cysteine residues, MT is capable of reducing Cu^{2+} to Cu^{+}, after which it can be coordinated with high affinity to MT.

As a reducing agent that readily coordinates Zn^{2+}, a proposed function of MT is sensing the presence of incoming oxidants. In this redox cycle, an ROS oxidizes MT leading to Zn^{2+} release.[49,69] This Zn^{2+} is responsible for upregulating Zn-dependent proteins through MTF-1. Either reduction of the previously oxidized MT with glutathione, or complete replacement with *de novo* MT then leads to a reestablishment of zinc homeostasis. In this manner, MT may either directly interact with the ROS, or in cases where ROS production is the result of a metal ion that readily coordinates MT, such as copper, MT may act to sequester the metal ion and effectively neutralize ROS activity.

III. Structural characterization

X-ray diffraction results have been reported from just two crystals, the first successful example was for rat Cd_5Zn_2-MT-2,[5] and the second was for yeast Cu_8-MT.[70] It should be noted that MT has been described as being notoriously difficult to crystallize, and much of our structural knowledge is the result of the many NMR-based studies reported. Structures based on analyses of the NMR data have been reported from several mammalian sources.[71–74] These structures provide the absolute connectivities of all atoms and their spatial relationship with the metal–thiolate core but not the alignment of the linkage between the two domains. The domain alignments were determined from the X-ray diffraction studies for the rat liver Cd_5,Zn_2-MT.[5] In the case of the X-ray crystal structure of rat Cd_5Zn_2-MT-2 species, all metal centres were tetrahedrally coordinated by cysteinyl-thiolates; later, when compared to the NMR structure, both showed identical molecular architectures.[75] A comparison of the NMR-based structures of human Cd_7- and Zn_7-MT-2 has shown overall maintenance of cluster geometry and demonstrated that MT can accommodate metal ions of varying size.[76] The ability of Cd^{2+} to replace Zn^{2+} isomorphously is exploited in many experiments due to several advantageous properties of the cadmium–thiolate cluster, such as the availability of $^{113/111}Cd$ NMR active isotopes, as well as the red shifted ligand-to-metal charge transfer band in the optical spectrum.

Copper(I) is capable of coordinating with a range of geometries depending on the Cu(I) : MT stoichiometric ratio. Digonal and trigonal geometries were found in the X-ray diffraction structure of the Cu-MT from yeast.[70] While no mammalian Cu-MT

X-ray diffraction structure exists, spectroscopic data have demonstrated the existence of both a Cu_{12}-MT and a Cu_{15}-MT for the two-domain, rabbit liver MT 2a, the former likely being mainly copper coordinated in a trigonal geometry, while the latter is likely a mixture of trigonal and digonal geometries.[77] In addition to these fully metallated structures, a copper folding intermediate in the β-domain, Cu_4-MT, has been isolated for both rat liver MT-1 and mouse MT-3 but is of unknown coordination geometry.[78] It is probable that this intermediate is related to the mixed metal species, Cu_4Zn_4-MT-3, thought to a critical product in controlling the oxidative damage caused by the Cu^+/Cu^{2+} redox cycle in Alzheimer's disease.[79] Previous NMR metal exchange experiments, in which Cd^{2+} was reacted with calf liver Zn_4,Cu_3-MT-1 and -2 have shown that cadmium ions could only displace the zinc ions.[15] Based on the NMR chemical shifts, it was concluded that these zinc ions were almost exclusively located in the α-domain, while the copper ions were located preferentially in the β-domain. From these results it has been proposed that MT is capable of separating metal types into different domains, essentially isolating the chemistry of both zinc and copper.

While NMR spectroscopy and X-ray diffraction studies have yielded the most significant information about the structure of MT, other techniques have also greatly contributed including CD, emission and Raman spectroscopy. In the case of CD spectroscopy, the ligand-to-metal charge transfer is strongly affected by the chirality of the protein and changes to the chirality can affect the signal observed.[80,81] For example, due to exciton coupling in mammalian MT, a typical spectrum has the cross-over of the derivative envelope centered at ~250 nm, however upon supermetallation exciton coupling is broken and a CD band maximum at ~250 nm is now observed.[82,83] In this way, one is able to infer that the metal coordination of both clusters is symmetric and that supermetallation results in a loss of this symmetry. Emission spectroscopy is also useful and in the case of copper emission is most intense when 12 equivalents of Cu^+ have been added forming Cu_{12}-MT. Loss of emission intensity past 12 equivalents of Cu^+ added to rabbit liver MT demonstrates that the protein is opening and assuming a less compact and more porous form.[84] Raman spectroscopy is also gaining interest because of its ability to determine the oxidation state of cysteine residues, the identity of coordinating ligands and finally identification of cysteine residues that could be modified by radical attack.[85] These techniques, while not as structurally specific as either NMR spectroscopy, X-ray absorption spectroscopic methods or X-ray diffraction studies, provide useful information that help in the determination of the dynamic structures of MT and further our understanding of its overall function(s).

IV. Metallation

Our understanding of the detailed functional dependence of MT as a metallochaperone relies greatly on our understanding of its metallation properties. Initial studies of both the metallation and demetallation reactions of MT led to hypotheses that metallation occurred in a cooperative fashion. In this scenario, the binding of one metal acts to facilitate the binding of further metals and, ultimately leads to MT existing as either apo-MT, or the fully metallated form. Three important consequences of the cooperative mechanism are (1) that partially metallated forms would not exist (only fully metallated and fully metal-free would exist), (2) that partially metallated forms of the protein would likely be too unstable to take part in cellular chemistry, and (3) that oxidation of the protein would lead to complete demetallation of the protein.

Recent mechanistic studies of Zn^{2+}, Cd^{2+} and As^{3+} binding to human MT have shown the mechanism of metallation to be in fact noncooperative.[57–59,86] In a noncooperative mechanism, metal binding events are independent of each other, so that: (1) partially metallated forms of the protein are stable, and could potentially take part in cellular chemistry, and (2) partial oxidation of the protein does not necessary lead to complete demetallation of the protein. Studies of the metal binding properties of human MT-2 with Zn^{2+} have shown a series of affinities that differ by four orders of magnitude (highest affinity $K = 10^{11.8}$, lowest affinity $K = 10^{7.7}$).[87] This range of association constants allows MT to act as a robust metallochaperone capable of accepting Zn^{2+} in cases of excess and donating Zn^{2+} in cases of deficiency.

1 General metallation properties of metallothioneins

We briefly summarize the major metallation properties of a range of MTs here, and below provide details. The most well characterized members of the MT family are the mammalian MTs (Fig. 1), which bind metals normally in two domains using 20 cysteine residues. Similar in number of coordinating cysteine residues (20) is the MT from the earth worm *Lumbricus rubellus*, which has been shown to possess three isoforms wMT-1, -2 and -3.[88,89] Interestingly, only wMT-2 appears responsive to cadmium ions.[90] The structure of wMT-2 has been proposed to be significantly different from mammalian sources of MT based on differences in CD spectra.[91] On the other hand, there are structurally distinct members of the MT family, such as the MT from seaweed *Fucus vesiculosus* (*f*MT). In the case of *f*MT a total of 16 cysteine residues are involved in metal ion coordination, and the protein is consider to bind copper *in vivo*.[92] No structural information is yet available for *f*MT. The extended linker of 14 amino acids has been proposed to separate a unique N-terminal γ-domain (7 cysteine residues) and a C-terminal β-domain (9 cysteine residues), both of which bind 3 Zn^{2+} and Cd^{2+} ions.[93]

The bacterial MT, SmtA, and the wheat E_c-1 MT are proteins with both cysteine and histidine residues used in metal ion coordination. In the first case, the bacterial MT SmtA binds four Zn^{2+} atoms through 9 cysteine and 2 histidine residues, which is thought to render one of the Zn^{2+} atoms inert to metal exchange allowing structural maintenance during metal depletion.[94,95] While in the second case, the β_E-domain of wheat E_c-1 contains two distinct metal binding clusters: the first which uses a combination of two cysteine residues and two histidine residues to coordinate 1 Zn^{2+} ion and a second which resembles a β-domain cluster.[96] The above examples highlight that by varying both the number and the type of coordinating amino acids, the MT family is capable of adopting a diverse array of structures.

The metal binding properties of the different MTs must reflect, in some way, the functions they serve. Because it has been very difficult to define these unique functions, the focus of much research has been on the individual metallation properties, the preferential binding of metals between the two domains, and particularly, on the stoichiometric ratios that appear to represent stable saturated clusters (the "magic numbers"). Clearly, in the absence of a straightforward relationship between the metallation status and function, emphasis must be placed on the structures formed during metallation, the mechanistics of metallation, and the possible reactivities of the protein as a function of metallation status.

MT appears exquisitely designed to bind the softer metals using the remarkably large number of cysteines in its sequence. The inorganic chemistry of metal–thiolate complexes provides many examples of metals ions binding with a combination of both terminal and bridging thiolates. As we will see below, MTs exhibit this same rich chemistry with a wide number of metals. In the following sections, we will be exclusively focusing on "magic numbers" of metallation of mammalian MT.

2 The "magic numbers" of MT

From the many analyses reported, we can summarise the "magic numbers", the thermodynamically preferred stoichiometries in the mammalian MTs, in terms of their coordination geometries:

(i) Tetrahedral coordination (MS_4), where four metals bind in the α domain and three metals bind in the β domain leading to metal–thiolate clusters (examples include Zn(II), Cd(II), and as well Fe(II) and Co(II)).

(ii) Trigonal coordination (MS_3), six metals bind in both α and β domains (consider as an example, Cu(I)).

(iii) Digonal coordination (MS_2), but here no well defined species have been reported from mammalian sources (examples include Cu(I), Ag(I) and even Hg(II)).

As we discussed above, our application of the term "magic number" is used to indicate the metal-to-protein (or metal-to-cysteine) stoichiometric ratios that, based on spectroscopic data, may represent a thermodynamically saturated complex. We can consider the saturation point to be associated with the formation of a specific structure—that structure is associated with a specific coordination geometry for the metal ion (4, 3, or 2 for the metals discussed here) and/or a unique wrapping of the peptide chain. The focus on a "magic number" has no importance unless one can extract information concerning the properties of the protein from those numbers. Considering that MT is concerned with metal binding on a larger scale than many other proteins, and for which a specific role of the bound metals is at the present time lacking, then the structural implications of the metal to protein stoichiometric ratios are significant.

3 What happens as the metal : MT ratio increases?

We turn now to the structural effects expected as the metal : MT ratio increases during metallation. Initially, addition of metal ions results in the formation of isolated metal–thiolate units. Following the formation of these isolated units, MT may accommodate more metals by increasing the complexity of the metal–thiolate cluster through an increase in the fraction of bridging sulfurs present. Often these bridging interactions do not alter the initial coordination geometry of the metal ions.

Following cluster formation, four scenarios are possible:

(i) Saturation: A metal : MT ratio is reached for which the addition of a single extra metal ion does not change spectroscopic or analytical data and it is inferred that there have been no structural changes. The metal–thiolate binding site does not accommodate additional metal ions. An example of saturation would be As^{3+} binding to human MT, where only six As^{3+} bind even when excess As^{3+} is present.[86] We associate these metal : MT stoichiometric ratios with 'magic numbers'.

(ii) Changes in the coordination geometry of the metal: The increase in the metal : MT ratio results in a change in the spectroscopic properties that can be associated with a change in the coordination geometry around some or all of the metals bound, the two-domain structure is maintained. An example of a change in coordination geometry would be the transition of Cu_{12}-MT to Cu_{15}-MT, where diagonal coordination is adopted to allow the extra metals to bind.[77]

(iii) Structural rearrangement of the peptide backbone: Increase in metal : MT ratio results in a major rearrangement of the binding site due to a change in the peptide chain wrapping. The protein rearranges changing the orientation of a number of cysteine residues and even the specific metal they bind. The realignment of the peptide chain is thermodynamically complicated because of the large numbers of thiols involved and is likely temperature dependent—with higher temperatures being needed. If spectral properties become more resolved at higher temperatures one might consider that the structure has been annealed. An example of this type of binding would be the binding of Cu^+ to Zn-MT as monitored through emission spectroscopy. At lower temperatures the binding is distributive with Cu^+ located in both the β- and α-domains, while at higher temperatures Cu^+ relocates to the thermodynamically favoured β-domain.[84]

(iv) Collapse of the two-domain structure: The final change that can occur following an increase in metal : MT ratio is more radical than the previous three. While the two-domain structure is characteristic of the mammalian (and other) MTs, there has been no compelling reason provided experimentally to support such a separation. Indeed, from the sequence one would not propose such a structure. In response to an increase in the metal : MT stoichiometric ratio we propose that collapse of the two-domain structure can lead to a single domain structure accommodating more metals, or alternatively two domains intimately connected by a shared metal ion that is coordinated to cysteine thiolates in each domain. In both models, the two domain nature of the metallothionein metal binding site is lost. We will propose below that the conversion of the independent two-domain motif to a single domain motif in mammalian MTs is associated with supermetallation. While the additional Cd^{2+} is initially limited to the two-domains, the modelling described at the end of the paper shows, not unexpectedlly, that the whole metal binding site reorganizes losing the two domain nature and adopting a single domain structure. The incoming Cd^{2+} is no different than the other seven at this point. An example of this type of binding is the

supermetallation of MT, in which a single Cd^{2+} binds to Cd_7-MT-1 or -3.[82,83,97]

As can be seen, the discussion above assumes that there may be several steps in the complete saturation of the MT binding sites. Therefore, our discussion about the concept of "magic numbers", and later "supermetallation", requires a decision on the mechanism of the metallation of MTs. A proper mechanistic understanding is critical because of its implications in the possible metallation status of the protein *in vivo*, particularly when considering the existence intermediates.

4 Noncooperative metallation of MTs

Although a number of studies since the 1970s have alluded to a cooperative mechanism of metallation, in which binding one metal triggers the formation of the completely saturated

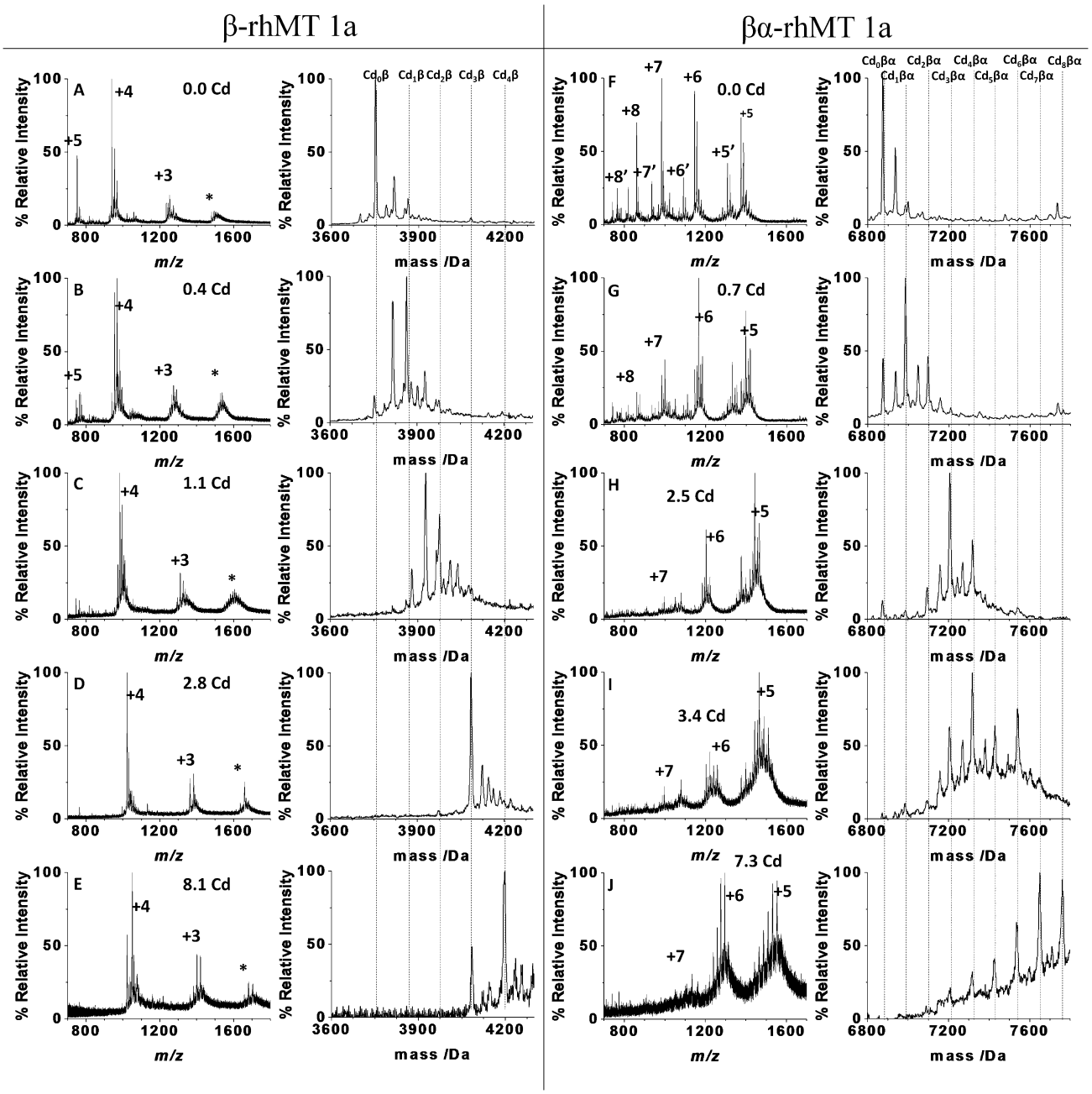

Fig. 2 Stepwise metallation of β-rhMT 1a and βα-rhMT 1a. ESI mass spectra recorded during the titration of apo-β-rhMT 1a (Left) and apo-βα-rhMT 1a (Right) with $CdSO_4$. Spectra of β-rhMT 1a (A–E) and the respective deconvoluted spectra were recorded at molar equivalents of 0.0, 0.4, 1.1, 2.8 and 8.1. Spectra of βα-rhMT 1a (F–J) and the respective deconvoluted spectra were recorded at molar equivalents of 0.0, 0.7, 2.5, 3.4 and 7.3. The * refers to a $+5$ m/z charge state from a small fraction of a species corresponding to slight dimer formation of β-rhMT, while the second set of charge states $+8'$ to $+5'$ represents a truncated version of βα-rhMT 1a. The protein used was recombinant human MT 1a. Adapted from Sutherland and Stillman with permission from Elsevier.[57]

binding site, recent experimental data does not support this. Rather, the recent data support a noncooperative mechanism that involves metals binding with a decreasing affinity for the protein. Thus, the experimental data show that for the MT proteins studied, metal binding is by way of a noncooperative mechanism, where the binding of each metal is essentially independent of the binding of previous ones. (This is not quite true, the successive metals are fully thermodynamically 'aware' of the previous metals because the binding sites have been used.)

A significant problem with studying metallation reactions with metals that are biologically relevant to the chemistry of MT, such as Zn^{2+}, Cd^{2+} and Cu^{+}, is that these are d^{10} metals, and consequently are chromophorically silent in many spectroscopies. In such cases, researchers have, until recently, been limited to the ligand-to-metal charge transfer bands in the optical spectrum (using absorption, emission, CD and MCD techniques) making their coordination properties difficult to study. One way to overcome this problem, involves using Co^{2+} as a spectroscopic probe for Zn^{2+}. The metallation of apo-MT to form Co_7-MT is of interest, because the results indicate that for the binding of at least the first three Co^{2+} atoms, the spectroscopic signature indicates the presence of isolated Co-tetrathiolate units within the MT binding site. As further Co^{2+} is added, both electronic absorption, EPR and ^{1}H NMR spectra indicate thiolate bridging occurs[98,99] as the coordination remains tetrahedral by sulfur. These results are significant in that if MT were to bind metal ions in a cooperative fashion then cluster formation would be immediate upon addition of Co^{2+} leaving a significant fraction of the protein in the unmetallated apo-MT state. The experimental data indicate that cluster formation requires the addition of several equivalents, and consequently MT binds Co^{2+} in a noncoooperative manner.

Recently, the technique of ESI-mass spectrometry, which detects each unique protein species with a different mass-to-charge ratio, has allowed the study of dilute protein solutions as a function of metal loading; data that complements the optical spectroscopic data. The recent mass spectral studies have demonstrated that the metallation of both human MT-1 and MT-3 proceed in a noncooperative manner for a variety of metals[40,57–59,86] and it is also likely to be the case for MT-2 and MT-4. Of the noncooperative isoforms studied experimentally, MT-1 has been more extensively analyzed, with noncooperativity shown for both the isolated β- and α-fragments, as well as the full βα-protein.[57,58] A graphical summary of the titration of the isolated β-fragment and the complete, two-domain protein of MT-1 with Cd^{2+} is shown in Fig. 2. From the observed charge states (A–E for β- and F–J for βα-) and their corresponding deconvoluted spectra, one can clearly see the stepwise formation of partially metallated (β- <3 and βα- <7 Cd^{2+}) species until saturation occurs upon addition of stoichiometric amounts of Cd^{2+}. While not shown for the sake of brevity, the titration of the isolated α-fragment proceeds in a similar manner.[58] The titration of apo-β-rhMT-1 with Cd^{2+}, and subsequent formation of both Cd_3-β-rhMT-1 and Cd_4-rhβ-MT-1, is illustrative of the characteristic "magic numbers" complexes of metallation.

5 Consequences of a noncooperative mechanism for metallation of MTs

The choice of mechanism profoundly alters our understanding of the function of MT as both an agent in responding to oxidative stress, and in maintaining metal ion homeostasis. As described above, a noncooperative mechanism supports the cellular involvement of partially metallated MT, which means that the recent studies reporting coexistence of metal free MT, both oxidized and reduced, with metallated MT,[49,100,101] can be rationalized as normal and expected properties of the protein.

Several MT polymorphisms have been linked to the longevity of certain human groups, with both low Zn-MT levels and satisfactory Zn^{2+} bioavailability being good markers for health.[102] Mutations of MT-1a (Asn27Thr) have also been associated with diabetes type 2 and cardiovascular complications,[103,104] where nitric oxide, an oxidizing agent, was used to determine the availability of Zn^{2+} from Zn-MT. Exposure of the mutant MT to nitric oxide, resulted in less Zn^{2+} release compared to the wild-type, suggesting that either the mutant is inherently less reactive, or that a large pool of partially oxidized MT exists. In both cases, the mechanism of metallation, and the potential for partially metallated species taking part in cellular chemistry has significant consequences in the understanding of the relationship between Zn^{2+} bioavailability, MT and the overall health of an individual. Specifically, if the mutant is inherently less reactive to NO, then one would predict the mutation has affected the most weakly bound Zn^{2+} ion. If, however, the protein is partially oxidized, then loss of Zn^{2+} from weakly bound sites would lead to an accumulation of Zn^{2+} in stronger binding sites. These strong binding sites would decrease cellular availability of Zn^{2+} and impede the health of the individual. It should be made clear that while this was an *in vivo* study and no information about the metal loading of the mutant MT is available, the final result of the individual is the same: only tightly bound Zn^{2+} exists and cannot be released easily either because of an increase in the stability of a weaker binding site, or partial oxidation and subsequent loss of a weaker binding site.

V. Detailed kinetic studies of the metallation of MT

While the above ESI-mass spectral studies show that Cd^{2+} binds to MT in a noncooperative manner, one must keep in mind that these structures represent thermodynamic minima, since the binding of either Cd^{2+} or Zn^{2+} to MT is complete within several milliseconds.[105] As a result, measurement of the kinetics of metallation has been somewhat limited to As^{3+}, which binds to three cysteine residues on the order of minutes, and Cu^{+}, which also binds to three cysteine residues within milliseconds, but whose structural rearrangement requires upwards of 20 min.[84]

1 Slow binding of arsenic to MT

To date, only the metallation by As^{3+} is sufficiently slow to allow analysis on a metal-by-metal bound basis using ESI-mass spectral kinetic analysis.[86,106,107] Of the four human

MT isoforms available, only MT-1 has been studied in this manner. In addition to human MT, As^{3+} binding to *Fucus vesiculosus* has also been reported.[108] The structure of $As(cys)_3$ is likely to be a triangular pyramid without bridging interactions. These studies of As^{3+} binding are likely to be a model for other metals because they definitively show the mechanism of metallation to be noncooperative and they also demonstrate metallation occurring as a series of sequential bimolecular reactions.

The As-metallation of human MT-1 shows that the rate of metallation is directly dependent on the number of available binding sites, with the isolated β- and α-domains binding As^{3+} the slowest and the genetically engineered triple-domain proteins (both ααα-MT-1a and βββ-MT-1) binding As^{3+} the fastest. We include the ααα and βββ data here because the As^{3+} binding kinetics confirmed that rates decreased as more As^{3+} bound and this likely is the same for other metals: the last metal binds with the slowest rate and lowest affinity. Fig. 3A shows the time resolution of the appearance and disappearance of the different As_n-MT-1a species. The data presented here show the time-resolved relative abundances of all the species measured continuously up to 7000 s. The smooth lines correspond to a model that uses only the initial concentrations of the apo-MT and As^{3+} in a multivariate fit connecting a series of sequential, bimolecular reactions to the experimental data. Fig. 3B clearly shows that the magnitude of

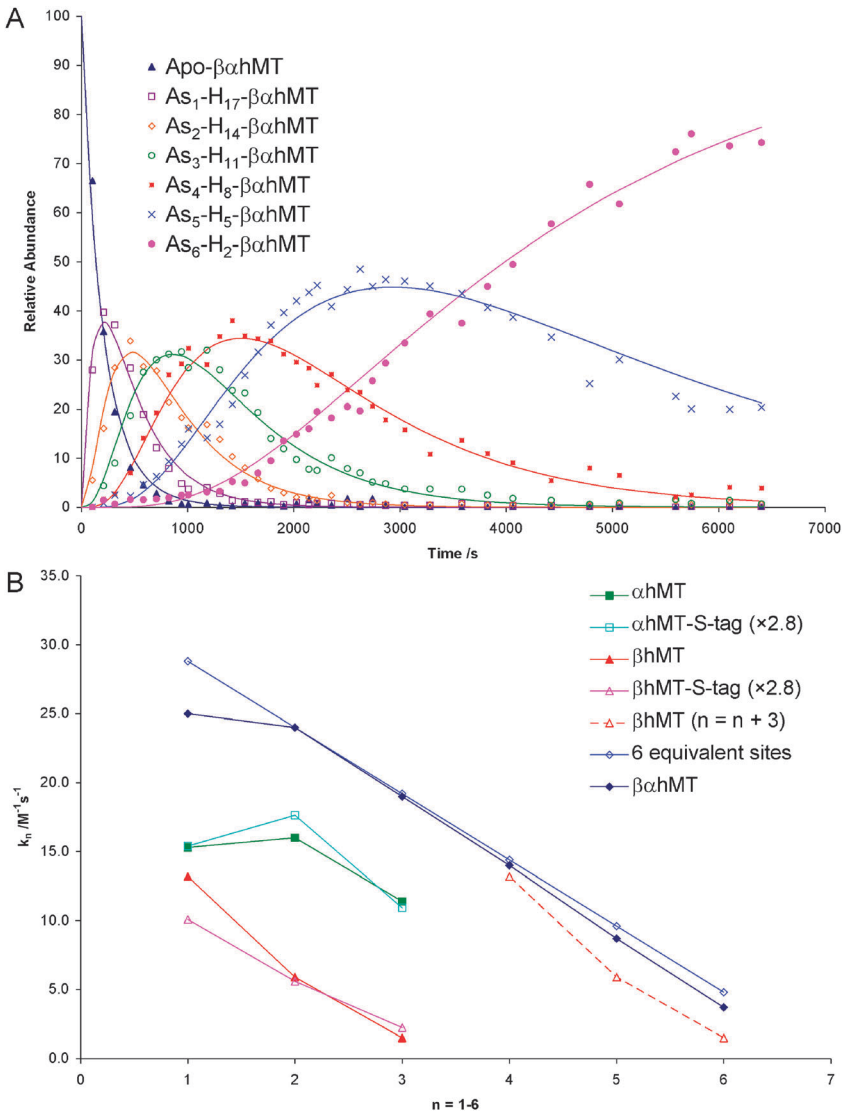

Fig. 3 (A) Time-resolved ESI-MS relative abundances human apo-βα-rhMT-1a following reaction with As^{3+} at 25 °C and pH 3.5 to form As_n-rhMT (n = 1–6). The reaction was carried out with an As^{3+} : MT stoichiometric ratio of 11 : 1. The relative abundances of each of the species are shown as the data points on the graph. The lines were calculated by fitting all the data to a series of sequential bimolecular reactions. (B) Comparison of the rate constants calculated from the time-resolved ESI-MS measurements for As^{3+}-metallation of α-rhMT-1a-s-tag, β-rhMT-1a-s-tag, α-rhMT-1a, β-rhMT-1a, the full protein βα-rhMT-1a and the trend in rate constant values for six equivalents sites where k_1 = 28.8 M^{-1} s^{-1}. The dashed line represents rate constant data for the β-rhMT-1a redrawn with the value of n shifted by three illustrate the similarity to the rate constant trend for the final three As^{3+} binding to the βα-rhMT-1a. The protein used was recombinant human (rh) MT 1a. Reproduced from Ngu *et al.* 2008 with permission from the American Chemical Society.[86]

the rate constants is directly dependent upon the number of available binding sites, where $n = 0$–3 for the isolated fragments and $n = 0$–6 for the two-domain βα-hMT-1a. The experiment was greatly extended by analyzing both temperature- and time-dependent ESI-mass spectral data recorded during the metallation reaction. The close fit to each set of data, and the ability to simulate the distribution of the As^{3+} at a specific time when added to a known amount of protein proved that for As^{3+} binding to MT, the overall metallation reaction proceeded as a series of sequential, irreversible bimolecular reactions, where As^{3+} binds to 3 cysteine residues. At equilibrium, and using substoichiometric As^{3+} equivalents, the stability of partially metallated As-MT species further emphasized the noncooperative nature of the metallation of MT.[107] One criticism of the original was that because the As^{3+} solutions were unstable at pH above 3.5, the binding was carried out at pH values that were of no biological relevance. However, in 2010 Ngu *et al.* reported that the As_6-βα-MT-1a was stable at neutral pH and more critically, could transfer As^{3+} to both apo-α-hMT-1a and apo-β-hMT-1a.[109]

2 Fast binding of copper to MT

Kinetic studies of Cu^+ binding to both Zn-MT 2 and apo-MT 1 have also been reported. These studies show that while Cu^+ binds very rapidly, the Cu^+ takes over 20 min to locate the thermodynamically preferred binding site. Both the relative change in emission intensity from Cu^+ to Cu^+ added and the time-dependent change in emission intensity is dependent on the exact sequence of the Cu^+ being added. In addition, kinetic studies show that the band maximum for the Cu-dependent emission also follows a trend with the sequence of the copper atoms number. More detail will be given in the copper MT section.

VI. Zinc and cadmium binding to MT

Zinc is critical to the continued health of an organism and is required for the proper functioning of a number of enzymes and transcription factors. With 5–20% of all cellular Zn associated with MT, structural motifs of Zn-MT are of critical importance.[110] Exposure of an organism to cadmium will negatively affect the health of an individual, including both liver and kidney damage. Cadmium is also a known carcinogen, capable of both inhibiting several DNA repair systems, as well as indirectly producing ROS to further DNA damage.[111,112] Perhaps the most well known disease associated with cadmium poisoning is Itai–Itai, made famous by mass cadmium poisoning in Toyama Prefecture, Japan, and most strikingly characterized by an increase in bone brittleness leading to an increased incidence of fractures.[113,114] While it may seem initially odd to include Zn^{2+}, an essential element, with Cd^{2+}, a toxic metal, both share similar coordination geometries. This is best demonstrated by NMR spectroscopy that has shown an almost identical protein fold when either metal is bound and a significant portion of the structural information known is derived from Cd-MT.[76]

For both Zn^{2+} and Cd^{2+}, the most well characterized form of MT is mammalian, with an N-terminal β-domain containing 9 cysteine residues and a C-terminal α-domain containing 11 cysteine residues. The traditional "magic number" for the full protein is 7 metal ions, 3 in the β-domain (Zn_3- or Cd_3-β-MT) and 4 in the α-domain (Zn_4- or Cd_4-α-MT). More recent evidence points towards a new supermetallated form of the protein that is discussed as the final section of this paper.

Several studies have together provided compelling evidence that the two domains of mammalian MT are structurally independent. To illustrate, the ^{113}Cd chemical shifts of the isolated α-domain are remarkably similar to those of the full protein indicating that the complete loss of the β-domain does not affect, to a large extent, the environment of the α-domain[115]. While NMR structural studies from several MT sources, including mouse[74] and human,[72] show a lack of interdomain NOEs, which would strongly suggest that the fully metallated domains are independent of each other. It is possible that he independence of the two domains is critical to the function of MT.

The initial proton NMR studies of MT demonstrated that in the absence of metal binding the structure was a random coil (although we note that proposed models of the apo-MT support the presence of a structural motif), however, upon addition of either Cd^{2+} or Zn^{2+} the structure became significantly more rigid.[116–118] Further analysis of the chemical shifts of cadmium atoms, as well as the splitting pattern, lead to the determination of the stoichiometry of the polynuclear clusters: Cd_3S_9 and Cd_4S_{11}.[115,119–122] Since these initial studies, solution structures have been determined from a number of MT sources including mammalian (human, rat, rabbit and mouse),[71–74,76] plant[96] and cyanobacteria.[123] The critical step in the determination of the overall structure of mammalian MT was the X-ray crystallographic[5] structure showing an identical molecular architecture to the previously determined NMR structure[75] but with the alignment of the two domains now defined.

VII. Copper binding to MT

Copper is vital for the continued health of all organisms. Copper induced toxicity is of considerable interest and its dyshomeostasis can lead to a number of diseases including Wilson's disease and Menkes disease.[44] Unlike zinc, free copper is redox active and able to catalyze the formation of hydroxyl radicals through Haber–Weiss and Fenton reactions.[42] A murine model of Menkes disease involving MT-1 and MT-2 null mice have shown enhanced sensitivity to copper toxicity.[46] In the case of Wilson's disease, a marked increase in Cu-MT has been demonstrated.[17,47] These two examples emphasize the importance of MT in maintaining health through the control of transient fluctuations in Cu^+ availability.[42,124]

In the case of copper, it has been reported that there exists a preference for its accumulation in the β-domain of mammalian MT before binding under thermodynamic control in the α-domain. In essence, this would allow simultaneous involvement of both Zn^{2+} and Cu^+ in the homeostatic functioning of the organism. This dual nature of the metal-binding properties of MTs could be critical to the brain specific MT-3 and its interactions with the protein $A\beta_{1-40}$-Cu^{2+}, a producer of reactive oxygen critical to Alzheimer's disease.[79,125] In this

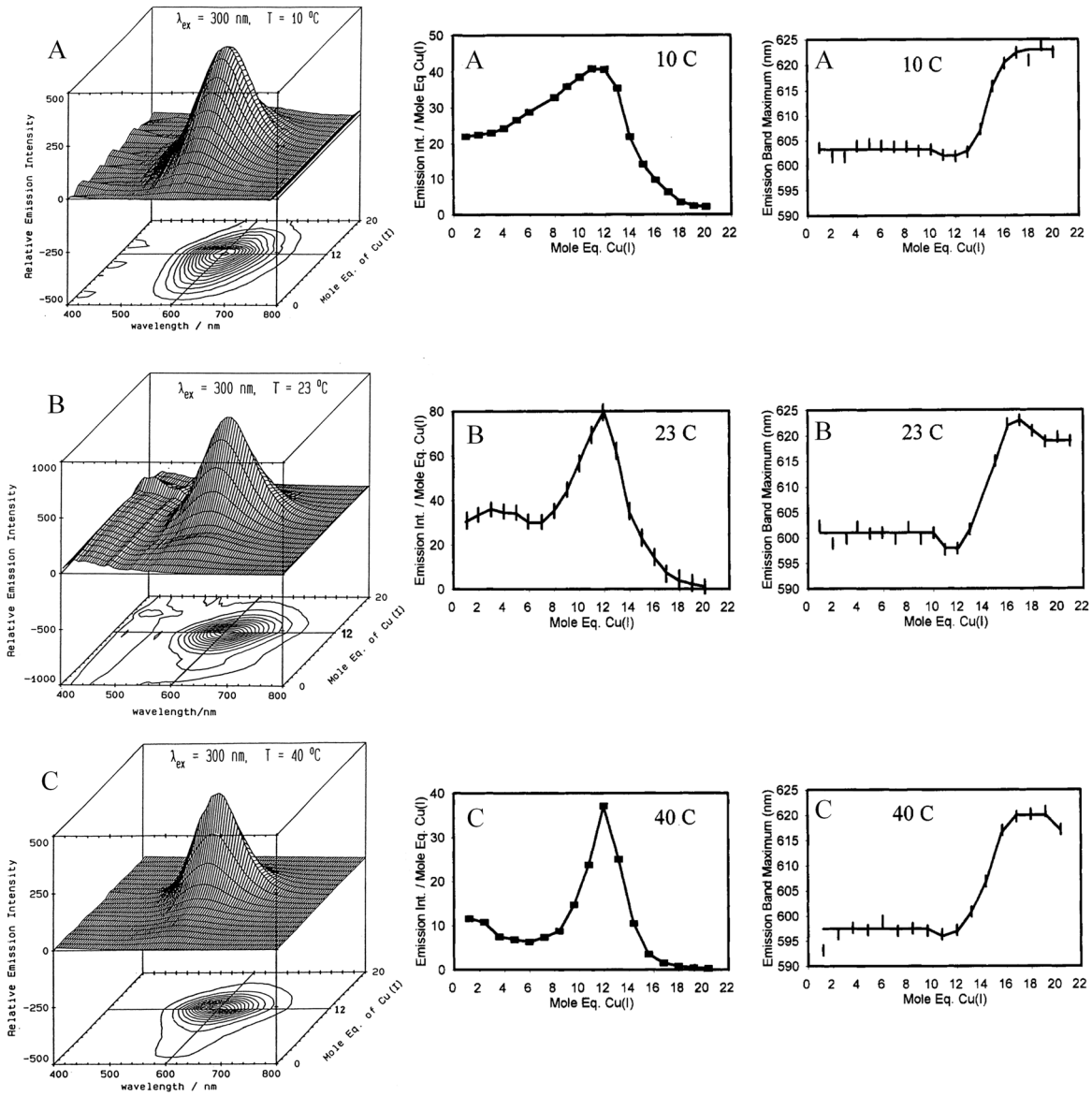

Fig. 4 The three dimensional plots located in the first column show changes in emission spectra as a function of Cu(I) : MT molar ratio for solutions of rabbit liver (rl) Zn-MT 2a, at 10 °C, 23 °C and 40 °C and a pH of 6.6. The grid line drawn across the contour diagram represents a Cu(I) molar ratio of 12, and the grid line parallel to the *z*-axis represents the 600 nm point in the spectra. The second column shows the normalized emission intensity (emission intensity at 600 nm divided by the Cu(I) molar equivalents) as a function of Cu(I) molar equivalents. In all cases maximum emission is observed upon formation of the fully metallated Cu_{12}-βα-rlMT 2a. It should be noted at this point that the absolute emission intensity represented here is in arbitrary units and direct comparisons between different spectra are not possible. Lower temperatures lead to a distributive addition of Cu(I), while higher temperatures result in preferential filling of the less emissive β-domain indicated by the reduction in normalized emission intensity between 4 and 6 Cu(I) added. The final column plots the location of the emission band maximum as a function of Cu(I) molar equivalents. The significant red shift of the maxima is the result of changes in coordination number as Cu_{12}-βα-rlMT 2a is converted to Cu_{15}-rlβα-MT 2a. Adapted from Green *et al.* with permission from the American Chemical Society.[84]

fashion Zn_7-MT-3 is capable of deactivating $A\beta_{1-40}$-Cu^{2+} by exchanging Cu^{2+} for Zn^{2+}. Following this exchange Cu^{2+} is reduced and sequestered specifically into the β domain of MT-3.

Emission spectroscopy has been particularly useful in studying Cu^{+} binding to MT. The first such study was for the fungus *Neurospora crassa*.[126] Since this initial study, both equilibrium and kinetic emission data have been reported for both Cu^{+} and Ag^{+} binding to different MTs. In these studies, excitation of Cu^{+} at 300 nm leads to a spin forbidden transition of $3d^{10} \rightarrow 3d^{9}4s^{1}$, or alternatively $3d^{10} \rightarrow 3d^{9}4p^{1}$, with subsequent emission from a long-lived state at a wavelength significantly red shifted from the initial excitation band (near 600 nm for Cu^{+} and 570 nm for Ag^{+}). Because the emission intensity is dependent on the environment of the metal ion, any changes in this intensity as a function of metal stoichiometry is the result of the dynamics of protein folding. In particular, the phosphorescent intensity is significantly impacted by the presence of either or both of dioxygen and water. In the absence of dioxygen, changes in

emission intensity as a function of metal loading indicate changes in the porosity of the metal–thiolate binding site that has been interpreted to indicate an expansion of the binding site.

The spectroscopic data (absorption, CD and emission) indicate that for the two-domain βα-MT-2a protein that there exist two significant saturation points, the "magic numbers" of copper binding, with Cu : MT ratios (i) of 12 and (ii) of 15.[77] Each domain is independently capable of binding 6 Cu^+ ions leading to the formation of metal clusters with the stoichiometry Cu_6S_9 and Cu_6S_{11} for the β- and α-domains, respectively.[127,128] Domain mixing experiments have shown the fluctionality of these clusters as Cu^+ ions located in the α-domain migrate to the β-domain displacing metal ions of weaker affinity in the process. Interestingly, the emission of Cu_{12}-βα-MT formed by the stepwise addition of Cu^+ to a solution of Zn_7-βα-MT is very time and temperature sensitive.[77,84] These results demonstrate that the initial Cu^+ binding is distributive without particular preference for either the α- or β-domain, which is the kinetic product of metallation. Given sufficient time and thermal energy, rearrangement of the protein leads to preferential accumulation of Cu^+ in the β-domain.

In detail, the metallation reaction of Zn_7-βα-MT with Cu^+ to form Cu_{12}-βα-MT can be seen in Fig. 4. This experiment was conducted at a number of temperatures, and in each case, a maximum emission at 12 molar equivalents of Cu^+ added was observed. Also important to this experiment is the preferential binding of Cu^+ to the β-domain of MT, which has been shown through both domain mixing experiments[127] and through proteolytic studies.[129] In the first stages of the metallation with Cu^+ : MT ratios of 1 to 7, the emission intensities are highly temperature dependent (Fig. 4). At 10 °C the increase in emission intensity is fairly linear, which is in complete contrast to the intensity dependence on the Cu^+ : MT ratios for metallation at 40 °C, where the emission intensity decreases as the Cu^+ : MT ratio increases. At lower temperatures, the increase in emission is resulting from distributed filling of both domains and is considered the kinetic product. Whereas at higher temperatures, it was suggested that the Cu^+ is sufficiently mobile to relocate to the less emissive β-domain,[127] which is considered to be the thermodynamically controlled domain specific product. As the titration proceeds with the Cu^+ : MT ratio increasing from 8 to 12 Cu^+ : MT equivalents, the emission from the experiments carried out at 10 °C continues to increase in a linear manner indicating distributive filling of the cluster. While the experiment carried out at 40 °C results in a sharp increase in emission intensity up to the maximum for a Cu^+ : MT ratio of 12, which is the result of exclusive filling of the more emissive α-domain. Regardless of temperature, all species were maximally emissive at 12 eq. Cu^+ added and significantly, further equivalents of Cu^+ resulted in a sharp decrease in intensity.

In the CD spectra, a mixed metal intermediate is formed (but only clearly at high temperatures) with a stoichiometry Cu_9Zn_2-MT, before Cu_{12}-MT forms and subsequently, Cu_{15}-MT, forms.[77] It was proposed that this Cu_9Zn_2-MT 2 species involved 6 Cu^+ in the β-domain, and two Zn^{2+} and three Cu^+ ions in the α-domain.

The band centre of the emission band near 600 nm is also dependent on the Cu^+ : MT ratio. The data in Fig. 4 show that (1) there is a slight blue shift upon formation of Cu_{12}-MT and (2) addition of Cu^+ after formation of Cu_{12}-MT leads to a significant red shift in the maxima. In the first case, the thermodynamically stable Cu_{12}-MT structure has a lower electronic ground state energy resulting in a blue shift of the band maximum. The second observation suggests the structure opens to accommodate more Cu^+ ions. This has been confirmed by CD spectroscopy, where further titration of Cu^+ results in the formation of a structurally unique Cu_{15}-MT band at 335 nm (+). This new structure is likely a mixture of both trigonal and digonal Cu^+ coordination environments. Further addition of Cu^+, in excess of 15 equivalents, results in an unfolding of the protein, which is seen by the loss of chirality in the CD spectra.

An unusual species was identified during titrations of Cd_7-MT 2 with Cu^+. The spectroscopic maxima were found for a mixed metal species with 12 Cu^+ and four Cd^{2+} Cd_4Cu_{12}-MT. It was proposed that the 4 Cd^{2+} were mixed with 6 Cu^+ in the α domain and the remaining 6 Cu^+ were bound in the β domain.[77] Like Hg_{18}-MT 2 (see below), it is possible that this species is in fact a single domain species.

To summarize, "the magic numbers" of the metallation of MT with Cu^+ are 6 for the isolated β- and α-domains and 12 and 15 for the full protein. When multiple metals are present both Cu_9Zn_2-MT and $Cu_{12}Cd_4$-MT form. Interestingly, Cu^+ has a preference of the β-domain, which has been used to successfully interpret the location of Cu^+ in many of these species.

While the data described above are essentially determined from equilibrated solutions, the thermodynamic products, the real key to understanding the metallation properties of all the MTs lies in the metallation and subsequent demetallation mechanisms. Kinetic analysis can provide mechanistic information. The few studies reported include competitive demetallation studies and Cd^{2+} binding to Zn-MT primarily from the Petering group,[105,130,131] as well as both copper and arsenic binding studies from the Stillman group.[77,86,106–108,127,132,133]

VIII. Mercury binding to MT

Mercury has no known physiological role and environmental exposure can come in several forms including elemental mercury (Hg^0), inorganic mercury (Hg^{2+} and Hg_2^{2+}) and organic forms of mercury, such as methylmercury (CH_3Hg^+), and toxicity is greatest for the alkylated species. Mercury has long been associated with MT, with early copurification attributed, in part, to the therapeutic use of mercurials.[36] MT-null mice have been instrumental in demonstrating the protective role of MT against Hg induced toxicity.[134–137] It should be noted that like CH_3Hg^+, Hg^0 is lipid soluble and can cross the blood brain barrier, where it can be oxidized to Hg^{2+} with catalase and H_2O_2.[138] MT has a critically important role in protecting an organism against methylmercury poisoning, and pretreatment experiments in which administration of MT inducers (Zn^{2+} and Cd^{2+}) caused an increase in the tolerance of astrocytes against toxic methylmercury insult.[56,139,140] The above examples highlight the importance of MT in the maintenance of neurological health.

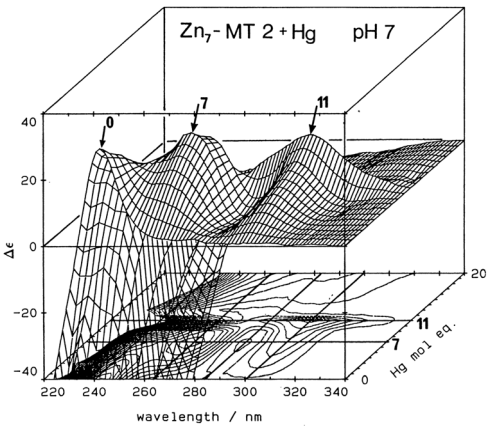

Fig. 5 Formation of rabbit liver (rl) Hg_7-rlMT 2a and Hg_{11}-rlMT 2a. The three dimensional projection has three maxima for 0, 7 and 11 equivalents of Hg : MT, which respectively represent Zn_7-rlMT 2a, Hg_7-rlMT 2a and Hg_{11}-rlMT 2a. The z axis is plotted in units of the Hg^{2+} added to the solution of Zn_7-rlMT 2. The grid lines added to the contour diagram are drawn for Hg^{2+} molar ratios of 7 and 11 and indicate 285 and 300 nm. From 0 to 7 equivalents of Hg^{2+} the spectral intensity increases in magnitude at 262, 282 and 297 nm with isodichroic points at 250, 278 and 289 nm. As Hg_{11}-rlMT 2a forms, the spectral intensity decreases in the 260 nm region and increases in the 300 nm region with maximal intensity observed for Hg : MT = 11. Hg : MT equivalents of 12 or greater at pH 7 in the absence of free chloride anions led to a featureless spectra indicative of a completely unwound protein. Reproduced from Lu and Stillman 1993 with permission from the American Chemical Society.[141]

A significant body of work has been produced describing not only the structurally significant stoichiometries of Hg-MT, but also the factors that influence their formation, such as time, temperature, presence of MT coordinated metals and the identity of the counter ions used in Hg^{2+} addition.[141–144] Four saturation points have been spectroscopically observed including Hg_7-, Hg_{11}-, Hg_{18}-, and Hg_{20}-MT. The latter, having a very weak CD spectrum, is likely the result of a complete unwinding of the protein leading to a random coil with Hg^{2+} coordinated in a linear fashion. The most notable technique used in titrations of MT with Hg^{2+} to date is CD spectroscopy. The technique measures the difference in absorbance between left and right circularly polarized light caused by the chirality of the chromophore. In this case, the chirality of the ligand-to-metal charge transfer of each mercury-thiolate cluster is measured. Because the metals that bind MT form predefined structures that exhibit specific chirality, CD spectroscopy is extremely sensitive in monitoring the metallation of MT. The CD bands specifically probe the metal-cysteine binding site structure because the chirality arises from a combination of the chiral wrapping of the peptide chain around the binding site and the exact energy of the LMCT band. The energies of the LMCT depend on the coordination number of the Hg^{2+} and, therefore, on the structure adopted at a each specific Hg : MT stoichiometric ratio. Changes in the wavelength of bands and the band morphologies in the CD spectrum as a function of Hg^{2+} loading indicate changes in binding site geometry as a function of the Hg^{2+} stoichiometric ratio.

While the metallation reactions of MT by Hg^{2+} have been studied for apo-MT, Zn-MT and Cd-MT, the importance of MT in zinc chemistry suggests that the displacement of Zn^{2+} by Hg^{2+} in MT is the most biologically relevant. Before a detailed analysis of the metal replacement of Zn-MT is described, it should be noted that: (1) displacement of Cd^{2+} in Cd-MT is the result of a distributive metallation, in which Hg^{2+} binds statistically to both the β- and α-domain, and (2) the metallation of apo-MT with Hg^{2+} follows a very similar pattern to that measured when Hg^{2+} is added to Zn-MT with the singular exception that in the early stages of the reaction the CD spectrum of partially metallated apo-MT has a broad peak at 270 nm (+) attributed to the formation of isolated $HgSR_4$ units.

The CD spectra recorded during the metallation reaction of Zn_7-βα-MT-2 with Hg^{2+} clearly shows three maxima: at 0, 7 and 11 equivalents of Hg^{2+} (Fig. 5).[141] These maxima correspond to Zn_7-βα-MT-2, Hg_7-βα-MT-2 and Hg_{11}-βα-MT-2, respectively. Molar ratios of Hg : MT between 0 and 7 result in a decrease in the band associated with the ligand-to-metal charge transfer of Zn_7-βα-MT-2 at 242 nm (+) with concomitant increase in the bands 262 (+), 285 (−) and 300 nm (+). S L-edge XANES support the similarity in structure between Zn_7-, Cd_7- and Hg_7-βα-MT-2, however in the latter case metal coordination is not identical and a mixed geometry structure may well exist.[145] Interpretation of EXAFS data suggests that a distorted tetrahedral coordination geometry of each Hg^{2+} is present, with two short and two long Hg–S bonds. It was proposed that this unusual coordination results from the structural stress of inserting the larger Hg^{2+} atoms into the cluster.[146] Between 7 and 12 equivalents of Hg^{2+} added, the CD bands 240 (+) and 262 nm (+) decrease in intensity, while 300 nm (+) broadens and intensifies at $Hg^{2+} > 9$ and is associated with a trigonally coordinated Hg_{11}-βα-MT-2 complex. At 11 Hg^{2+} equivalents, a complete replacement of all other spectral features with 300 nm (+) occurs. When 12 and greater equivalents of Hg^{2+} are added, the 300 nm (+) peak steeply decreases. This quenching of the CD spectrum suggests that Hg_{20}-βα-MT-2 forms through the opening of the structure.

Hg_{18}-βα-MT-2 from rabbit liver has been reported to be a structurally significant species (Fig. 6), where it was proposed that each Hg^{2+} atom adopts a pseudotetrahedral structure, each with two bridging thiolates and outlying chloride anions.[142,144] The necessity for Hg^{2+} to be coordinated to two cysteine residues and chloride ions has been confirmed by XAFS measurements.[146] In this way, each Hg^{2+} atom is effectively stacked on the others leading to the formation of one large domain instead of two smaller ones. Interestingly this species may only be formed from isoform 2, unless isoform 1 is first lyophilized and then dissolved in acid. Formation of Hg_{18}-βα-MT-2 has been attributed to residues 38–40, where the unique presence of two consecutive proline residues allows the twisting of the protein to accommodate a single domain structure. In the case of lyophilized protein, breaking of the solvent-protein bonds allows an alternate conformation to be adopted in acid, which upon addition of Hg^{2+} leads to the formation of Hg_{18}-βα-MT-1. We will return to the formation of this single-domain species below, but to

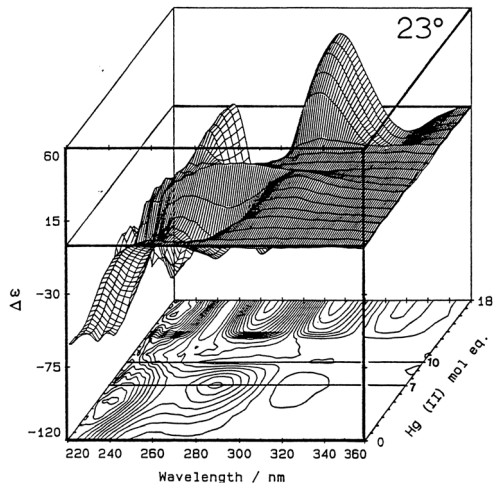

Fig. 6 A 3-dimensional representation of the formation of rabbit liver (rl) Hg_{18}-rlMT 2a using CD spectra recorded during a titration of a single sample of apo-rlMT 2a with Hg^{2+} at pH 2 and 23 °C in the presence of chloride anions. The *z*-axis is the Hg : MT molar ratio for the Hg^{2+} added to a solution of apo-rlMT 2a held at pH 2. Trace 1 is for 0 Hg^{2+} added; trace 19 is for 18 mol equiv of Hg^{2+} added. The final trace has a very strong intensity indicating that at 18 equivalents of Hg^{2+} added, the protein has adopted a novel chiral structure. No further changes in the CD spectrum were observed for Hg : MT = 18–40. Reproduced from Lu & Stillman 1993 with permission from the American Chemical Society.[142]

summarize the "magic numbers" of Hg^{2+} to MT binding are 7, 11 and 18.

IX. Supermetallation of MT

While we have discussed above the concept of "magic numbers" in the metallation properties of MTs, we have also noted that metallation past these maxima have been reported for several different metals. The fact that more metals can bind to any of the MTs beyond the number identified as normal is not surprising. MTs bind the typical metals of inorganic metal–thiolate clusters, with metal : cysteine ratios less than 1 (for example, 7 : 20), because of the high coordination numbers of the metals, 2, 3 and 4 being common for Ag(I), Cu(I), Hg(II), and Zn(II) or Cd(II). Saturation of the metal binding sites in MT may often be associated with the complete unfolding of the peptide chain, such as in the case of Cu(I) and Hg(II), which results in changes to the number of cysteine-based donor ligands. In the extreme just one cysteine residue would coordinate one metal ion, so the maximum metallated state for mammalian MT would be 20, that is metal : cysteine = 1. This is the basis of the silver quantitation test introduced by Cherian, namely, that excess Ag(I) will bind on a 1 : 1 basis with the cysteine residue, allowing analysis of the Ag(I) content to provide the MT content accurately.[147] On the other hand, supermetallation in the context of MT means the binding of a metal ion in excess of traditional levels that exhibits unique spectroscopic and structural properties. The examples described below are each recognized as supermetallated states by the appearance of new and specific spectroscopic parameters.

1 Supermetallation of the β-domain of MT with cadmium

A series of recent papers have greatly contributed to our recognition of a supermetallated motif in Cd-MT, and have outlined the unique spectroscopic properties of this additional metal binding site.[57,82,83,97] Extensive work by the Stillman group has demonstrated that supermetallation is capable not only in the full two-domain protein, but also in both the isolated β- and α-domain of human MT-1a. While a recent paper by Vasak and co-workers has demonstrated that supermetallation can also occur in the full two-domain protein of the brain specific MT-3. Supermetallation has also been observed in other kingdoms of life, *e.g.* plants.[148] Taken together, these results strongly suggest that supermetallation is a property common to many forms of MT.

Both the α-fragment and the β-fragment of MT-1 are capable of binding a single extra Cd^{2+} above the "magic numbers" of 4 and 3 respectively. We will describe first in detail the optical and ESI-mass spectral data that supports our proposal that these additional metal ions are indeed forming new species.

We begin with Fig. 7 in which the use of ESI-MS techniques to follow metallation of the β-domain of human MT-1 provides critical insight into the corresponding changes observed in both the UV absorption and CD spectra. Similar data have also been reported for titrations of the α-domain of human MT-1.[83] Fig. 7A and B show the deconvoluted mass spectra of Cd_3-β-MT and Cd_4-β-MT, respectively. The difference between 7A and 7B is a mass of 112 Da, or 1 Cd^{2+}, which is the result of the addition of 4.4 molar equivalents excess of $CdSO_4$. Fig. 7C and D show the UV and CD spectroscopic signatures of both Cd_3-β-MT and Cd_4-β-MT, respectively. In both cases, the data in 7C and 7D arise from the ligand-to-metal charge transfer band. While the UV absorption spectra did not change significantly, the CD spectra showed drastic changes in the extrema as a function of the metal loading. The maxima for Cd_4-β-MT was blue shifted from that of Cd_3-β-MT, likely the result of a breaking in exciton coupling between the three Cd^{2+} ions of the system as observed when Cd_5-α-MT is formed.[83] This significant change in the CD band envelope morphology provides strong support that the binding of the fourth Cd^{2+} atom directly involves the metal–thiolate cluster.

To clarify the location of the metal ion that results in the formation of the supermetallated Cd_4-β-MT and Cd_5-α-MT, we have used cadmium NMR spectroscopy. ^{113}Cd NMR data have allowed elucidation of the number of Cd^{2+} atoms in the metal–thiolate cluster and provided the likely identity of the type of ligands involved.[57,82,83,97] While initial Cd^{2+} titrations monitored by CD spectroscopy and ESI mass spectrometry provided the first evidence for supermetallation of the α-domain, and the β-domain, it was not until the direct 1-D ^{113}Cd NMR spectrum of these two domains that direct interaction with the metal–thiolate cluster was confirmed. We will describe the data for the β-MT-1 and the α-MT-1 species here. Both 1-D and 2-D NMR spectra are available for the isolated β- and α-domains, however we will discuss here only the 1-D spectra for the β-domain and the 2-D spectrum for the α-domain.

The NMR spectrum from the β-domain, Fig. 8A, shows a mixture of Cd_3- and Cd_4-β-MT. This mixture is the result of a

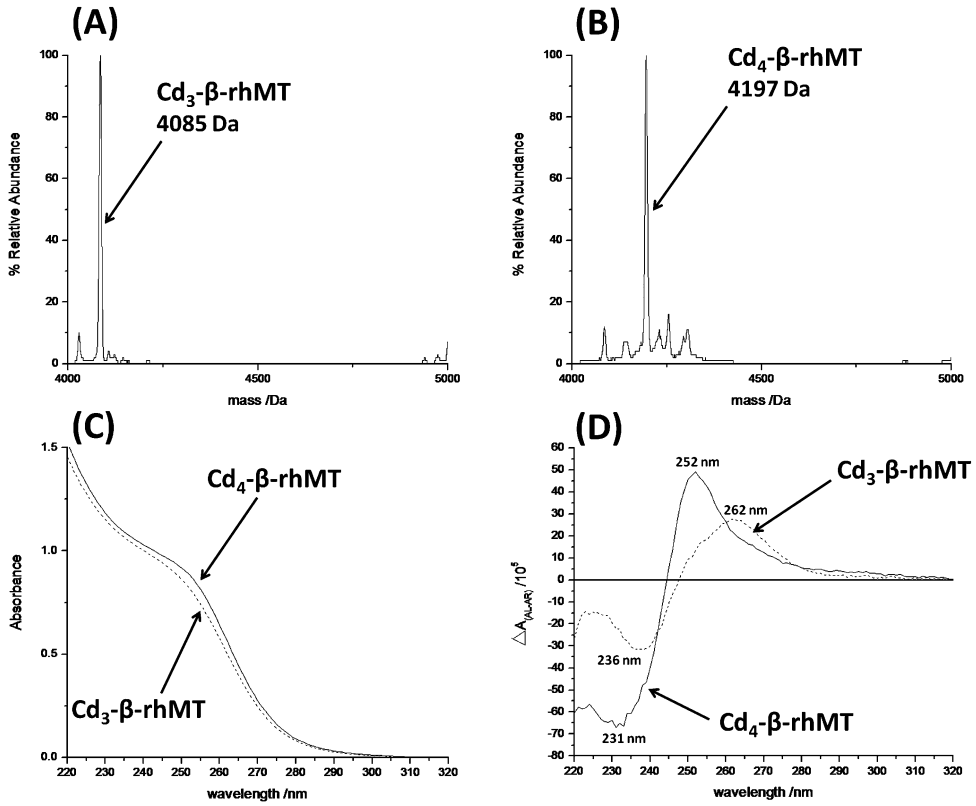

Fig. 7 Formation of supermetallated recombinant human (rh) Cd_4-β-rhMT 1a as monitored by ESI-MS deconvoluted spectra, UV absorption and CD spectra. (A) ESI-MS deconvoluted spectrum of Cd_3-β-rhMT 1a, showing the mass equal to the apoprotein with three Cd^{2+} ions. (B) ESI-MS deconvoluted spectrum of supermetallated Cd_4-β-rhMT 1a formed following the addition of a further 4.4 molar equiv of $CdSO_4$ to Cd_3-β-rhMT 1a, showing the additional mass from one extra Cd^{2+}. (C) UV absorption and (D) CD spectral changes observed for Cd_3-β-rhMT 1a and supermetallated Cd_4-β-rhMT 1a formed following the addition of a further 4.4 molar equiv of $CdSO_4$ to Cd_3-β-rhMT 1a. To ensure accurate speciation, the same samples of Cd_3-β-rhMT 1a and Cd_4-β-rhMT 1a were used in all experiments. Reproduced from Sutherland *et al.* 2010 with permission from the American Chemical Society.[82]

slight excess of $^{113}CdCl_2$ added to solution to stabilize MT against air oxidation. By adding an excess of $^{113}CdCl_2$, Fig. 8B shows only peaks associated with Cd_4-β-MT. In these two spectra, each peak falls between 600 and 700 ppm, a strong indicator that each cadmium centre is coordinated to only cysteine residues. The supermetallated cadmium atom has been tentatively assigned to the peak corresponding to 602.5 ppm, which would suggest tetrahedral coordination to four thiolates, or three thiolates and a single water molecule/chloride ion.

2 Supermetallation of the α-domain of MT with cadmium

In the case of the α-domain, more advanced ^{1}H-^{113}Cd techniques have allowed assignment of the possible connectivities of the supermetallated form of the α-domain, Fig. 9. This technique takes advantage of the ^{3}J scalar coupling constant between the cadmium ions and the β protons of the cysteine residues. In this way spectra may be acquired at a significantly faster rate (60 min *vs.* 60 h) than a traditional 1- or 2-D ^{113}Cd experiment, and in addition the spectra also provide the connectivities of the Cd^{2+} ions, which can lead to a fast assignment of the overall structure of the cluster. Because the signal associated with the supermetallated cadmium atom in the α-domain is significantly shielded at 224 ppm, it is likely that this centre corresponds to an octahedrally coordinated $Cd(RS)_2(OH_2)_4$ and is likely located near the cluster crevice, where a number of cysteinyl-sulfurs are exposed. Based on the chemical shift of the protons, this fifth Cd^{2+} ions is likely coordinated to cysteine residues 34 and 57.

3 Supermetallation of βα-rhMT with cadmium

The full human MT-3 protein has also been confirmed to supermetallate by 1-D ^{113}Cd NMR spectroscopy.[97] Most interestingly, in the case of MT-3, the addition of a single cadmium atom leads to a decrease in the Stoke's radius, determine through analytical size exclusion chromatography (SEC), which is a result of the protein assuming a more compact form. When supermetallation of the isolated domains reported for MT-1 is taken together with that of the full protein, it is quite likely that both domains are involved in coordination of the eighth metal ion. However, based on the location of the supermetallated chemical shifts observed for the isolated domains of MT-1 (602.5 ppm in the β-domain and 224 ppm in the α-domain see Fig. 10),[82,83] it is quite likely that the β-domain, with a more downfield supermetallated peak, donates more thiolates to stabilize the structure. Consequently, while both domains are capable of binding an additional metal ion, the bulk of the chemistry related to this new metal atom is likely associated with the β-domain.

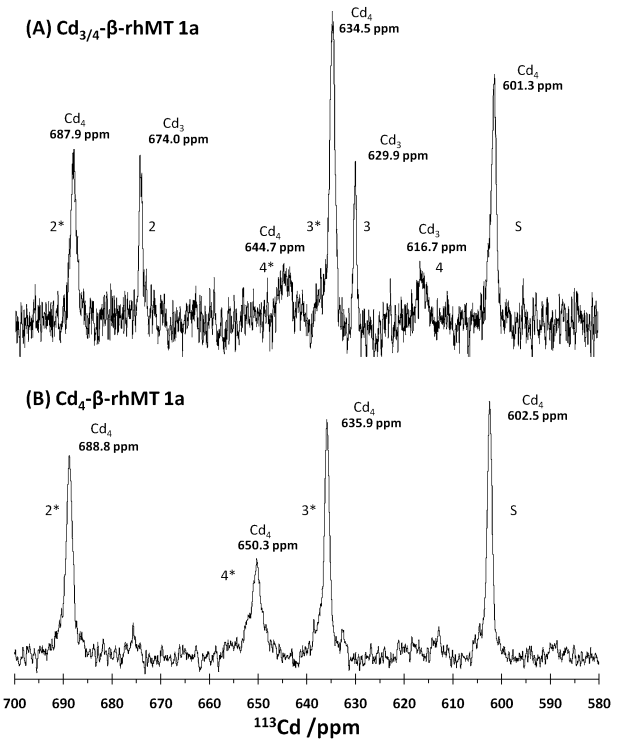

Fig. 8 NMR spectral characterization of supermetallated recombinant human (rh) Cd_4-β-rhMT 1a. Direct 1D $^{113}Cd\{1H\}$ NMR spectrum (133 MHz) of (A) a mixture of Cd_3-β-rhMT 1a and Cd_4-β-rhMT 1a and (B) Cd_4-β-rhMT 1a formed by addition of excess $^{113}CdCl_2$. Slight shifts in the values of Cd_4-β-rhMT 1a were observed between the mixture and the pure supermetallated sample. This shift is attributed to the addition of chloride ions from $^{113}CdCl_2$ to the solution and is most pronounced in the least intense Cd_4-β-rhMT 1a signal at 644.7 ppm, with a total downfield shift of 5.6 ppm. Reproduced from Sutherland *et al.* 2010 with permission from the American Chemical Society.[82]

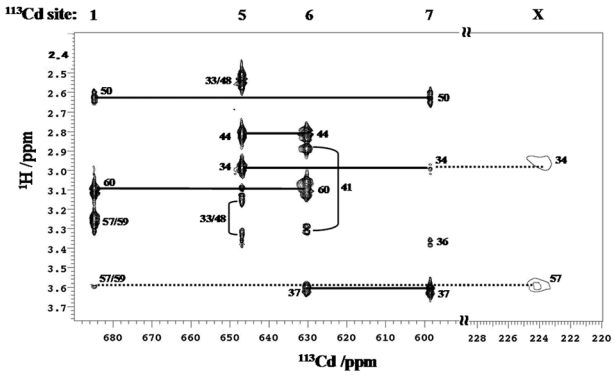

Fig. 9 Determination of the cysteine-cadmium connectivities in supermetallated recombinant human (rh) Cd_5-α-rhMT 1a. The figure shows a combination of two indirect 2D ^1H–^{113}Cd HSQC NMR spectra for isotopically enriched $^{113}Cd_4$-α-rhMT 1a titrated with an additional 10.0 molar equivalents of $^{113}Cd^{2+}$ to form the $^{113}Cd_5$-α-rhMT 1a species. The spectra were recorded in the ^1H chemical shift range 2.3–3.7 p.p.m. and the ^{113}Cd ranges 590–690 p.p.m. (^3J = 66 Hz) and 220–245 p.p.m. (^3J = 40 Hz). This two dimensional plot shows how the HSQC technique can determine the connection between individual cysteine residues (*y*-axis) and individual cadmium atoms (*x*-axis). When two or more cadmium atoms share one cysteine residue, two signals with similar ^1H chemical shift range will appear for multiple cadmium atoms. For example, the ^1H chemical shift labelled 50 at 2.6 ppm for both cadmium 1 and cadmium 7. The cadmium numbering scheme follows the original numbering scheme of Otvos and Armitage for the two-domain Cd_7-βα-MT 2a.[119] Reproduced from Rigby-Duncan *et al.* 2008 with permission from John Wiley and Sons.[83]

While no NMR data are currently available for the supermetallated form of the two-domain MT-1 (Cd_8-βα-MT-1), metallation studies involving ESI mass spectral data indeed indicate that Cd_8-βα-MT-1 forms. Interestingly, one would predict that since each domain is capable of independently supermetallating that the final product of a titration of apo-βα-MT-1 with Cd^{2+} would be Cd_9-βα-MT-1.[82,83] However, in a titration of apo-βα-hMT-1 with Cd^{2+}, Cd_n-βα-hMT-1 species with n = 1 to 8 were observed with stoichiometries that directly correspond to the amount of Cd^{2+} added to solution (Fig. 2). As with the titration of apo-β-MT-1 shown as Fig. 2, the m/z charge state spectra (F–J) and the corresponding deconvoluted mass spectral data recorded for species between apo-MT and the fully metallated Cd_7-βα-MT-1, are significantly complicated by the presence of several multiply metallated species. In terms of charge states, those for apo-βα-MT-1 range from +8 to +5 (F). When one equivalent of Cd^{2+} is added to solution both the +8 and the +7 charge states reduce in intensity (G) indicating a folding of the protein to a smaller volume triggered, which can no longer support the higher charge states,[149,150] by the addition of the first Cd^{2+}. Upon addition of a second equivalent of Cd^{2+} (H), the +8 charge state disappears. As Cd_7-β-MT-1 converts to the supermetallated Cd_8-β-MT-1, there is a slight increase in the +6 charge state relative to the +5, indicating that binding of the eighth Cd^{2+} leads to an expansion of the protein's volume (J). The final product of the titration is a mixture of Cd_6-, Cd_7- and Cd_8-βα-MT-1. With each of the two domains capable of supermetallation, it is likely that the binding affinity of the eighth Cd^{2+} involves both domains with significant contribution of cysteine residues from the β-domain. Although these experiments provide excellent stoichiometric information, NMR spectroscopy will be required to determine the identity of coordinating ligands as well as the effects of this eighth Cd^{2+} on the two domain protein.

One important aspect that must be examined further is the exact location of the lower-affinity binding site(s) on Cd_8-βα-MT(1 and 3). The NMR spectra of several species have been described including human Cd_7-βα-MT isoforms 1, 2 and 3, the two isolated fragments Cd_3-β-rhMT-1a and Cd_4-α-rhMT-1a, as well as their respective supermetallated counterparts (Fig. 10). This figure clearly shows that with the exception of the $^{113}Cd^{2+}$ supermetallated signal at 224 ppm in the α-domain of MT-1a, all other peaks are located between 600 and 700 ppm. Using this figure we can infer based on the available NMR data from the isolated domains that supermetallation will involve thiol ligands from both domains. Further these ligands will likely produce an NMR spectrum similar to a mixture of Cd_4-β-MT 1a and Cd_5-α-MT 1a with the sole exception of loss of the supermetallated peak located at 224 ppm for the α-domain since the eighth Cd^{2+} is likely to have a combination of cysteine residues from both domains. Consequently without prior knowledge of supermetallation,

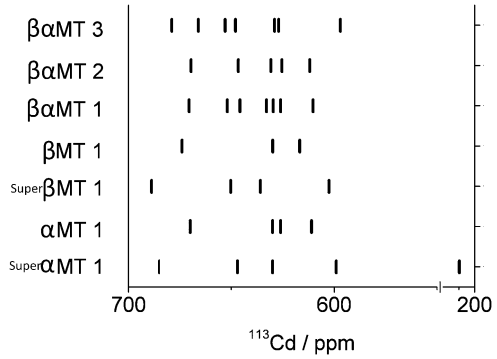

Fig. 10 Comparison of reported ^{113}Cd NMR resonances for human MTs: Cd_7-βα-rhMT-3, Cd_7-βα-hMT-2a, Cd_7-βα-hMT-1a, Cd_3-β-rhMT-1a, supermetallated Cd_4-β-rhMT-1a, Cd_4-α-rhMT-1a, and supermetallated Cd_5-α-rhMT-1a. This diagram highlights that with the exception of one peak in the supermetallated α domain, all signals fall within 600 to 700 ppm indicative of tetrahedrally coordinated cadmium-cysteinyl thiolates. We note that in this diagram, for the spectrum of Cd_7-βα-hMT-2a, the resolution precludes separation of overlapping resonance 1 and 2 (near 670 ppm) and 3 and 4 (near 645 ppm), so that in total there are seven resonances. In the MT nomenclature, h indicates that the source of MT was from a human, while rh indicates that while the protein is human in nature, it was isolated as a recombinant protein from a source other than humans. Reproduced from Sutherland *et al.* 2010 with permission from the American Chemical Society.[82]

provided by CD spectroscopy and ESI-mass spectrometry, one would assume that this extra peak is the result of sample heterogeneity and not in fact a new low affinity binding site.

If the structure of the supermetallated Cd_8-βα-MT species was dominated by the presence of the β-domain, then this would be critical to the overall function of MT in the body. Specifically, the β-domain of MT-3 has been shown to be critical to the overall function of MT-3 as a neuronal growth inhibitor.[151,152] MT-1 may also be altered to inhibit neuronal growth by the addition of Thr5, and by mutating both S6P and S8P, which is thought to increase cluster fluctionality. Based on these results, it becomes evident that β-domain-centred chemistry, which has not been well studied in an isolated form, may be critical to many functions of MT.

This additional metal could be an exchange intermediate essentially frozen by the higher binding affinity of Cd^{2+} compared to that of Zn^{2+}. The hypothesis proposed to account for the presence of the intermediate suggests that it represents the metallation/demetallation mechanism of apoenzymes, as well aiding in the sequestration of toxic metals with concomitant release of Zn^{2+} to upregulate the production of more MT. This proposal would imply that the extra metal is located on the outside of the cluster; however, there exists ambiguity in the exact location of the additional metal binding site. A computation model, Fig. 11, in which all eight Cd^{2+} ions are tetrahedrally coordinated to 4 cysteine residues leading to a complete collapse of the two-domain structure shows how this additional metal centre eliminates domain separation and would consequently allow for equilibration of the incoming metals with the two domains.

4 Supermetallation of βα-rlMT with mercury and copper

Cadmium-containing MTs have provided the most extensive set of data to support the proposal that supermetallation is possible and that these species are unique structurally. In the past, spectroscopic evidence for species heavily-loaded with metals was presented from CD titration data. These results were compelling at the time because the change in the optical data was sharp and very much dependent on the exact metal : MT ratio. The four examples that we wish to conclude this paper with are based on Hg^{2+} and Cu^{+} binding.

We have above described the formation of four unusual species, namely the Hg_{18}-MT 2, the Cu_9Zn_2-MT 2, the Cu_{15}-MT 2, and the Cd_4Cu_{12}-MT 2. Each identified from CD spectral titrations. At the time of their discovery ESI-mass spectral techniques were not available. The authors based their interpretations of the speciation on analytical data for the metals and on the dependence of the spectral changes on the metal : MT ratios. If the spectra changed steeply with each additional metal, then it was concluded that a single metal bound, because K_f must be a large number. We can interpret these results in terms of supermetallation, which is the formation of species with specific and well-defined structures. The problem at this time is obtaining structural information.

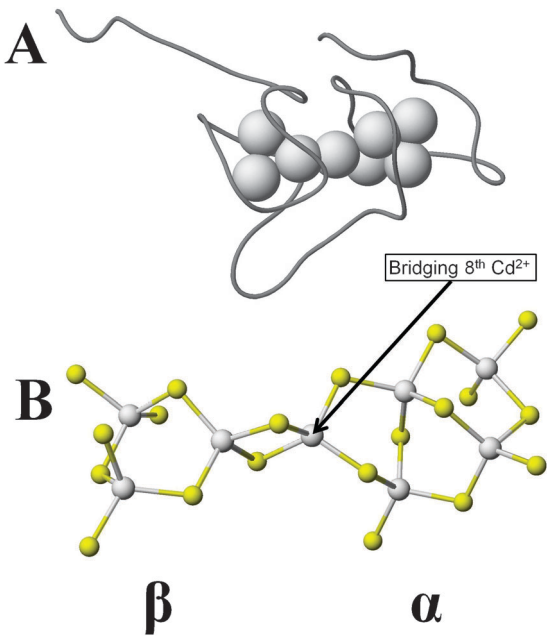

Fig. 11 Molecular model showing a possible structure for the supermetallated recombinant human (rh) Cd_8-βα-rhMT 1a structure. (A) Ribbon structure of the backbone of Cd_8-βα-rhMT 1a with the cadmium atoms represented as spheres calculated using a locally modified force-field with MM3/MD methods for molecular modelling. The N-terminal β domain is located on the left hand side, while the C-terminal α domain is located on the right-hand side. (B) The cadmium-cysteinyl-thiolate clusters of Cd_8-βα-rhMT 1a are presented as a ball-and-stick model: β domain (left) and α domain (right). The structure was created by inserting an additional Cd^{2+} ion between the two domains, and minimizing the structure in two steps: (1) 1000 ps at 500 K, and (2) 5000 ps at 300 K. The conformer with the lowest energy is presented above. The initial structure of the Cd_7-βα-rhMT 1a was provided by Chan *et al.*[153]

X. Conclusions

While the functions of MT are not known, MT is clearly intimately involved in metal ion homeostasis, in toxic metal detoxification, and as an agent to protect against oxidative stress. In order to further our understanding, research has focused on the metallation properties of MT and the "magic numbers" of metal binding, in other words the stable saturated clusters formed. To summarize these stoichiometries: the most well established for Zn^{2+} and Cd^{2+} of 7 in the mammalian protein, and for Hg^{2+} ratios of 7, 11 and 18, and for Cu^{+} ratios of 12 and 15. Supermetallation, a special "magic number" of metal binding, is metallation in excess of traditional levels that significantly alters the spectroscopic properties of the protein. In this case Hg_{18}-βα-MT 2, Cu_9Zn_2-βα-MT 2, Cu_{15}-βα-MT 2, Cd_4Cu_{12}-βα-MT 2, and Cd_8-βα-MT 1 and 3 are all thought to be supermetallated species. The most well studied member of the supermetallated family is Cd_8-βα-MT, which is proposed to be a metal exchange intermediate that has been effectively frozen by a combination of the high affinity of Cd^{2+} for thiolates and by the relatively high concentration of Cd^{2+} used (~4 molar equivalents *excess* per MT). Because each isolated domain is capable of supermetallation, a model was proposed in which the eighth Cd^{2+} atom coordinates to both domains leading to a loss of their unique identity. The merger of these domains and exchange of their respective metals may be critical in the production of thermodynamically stable products, such as isolation of Cu^{+} in the β-domain and Zn^{2+} and Cd^{2+} in the α-domain. Once the complete structure of Cd_8-βα-MT is known, it will become possible to model metal exchange reactions more accurately with the aim of describing the exact function of MT.

Acknowledgements

We gratefully acknowledge financial support from NSERC of Canada through a Canada Graduate Scholarship (DEKS), Discovery Grant and Equipment Grant (MJS). MJS thanks the many students who have worked on the metallothionein project for the last 20 years, most recently Thanh Ngu, Kelly Duncan, Jayna Chan, Maria Salgado, Janice Lee, Tyler Pinter, and Maureen Merrifield. We wish to acknowledge the contributions of Dr Peter Kille (Cardiff) in providing the initial protein constructs for our work and Mr Doug Hairsine provided excellent technical assistance with the mass spectrometry.

Notes and references

1 Y. Kojima, in *Methods in Enzymology: Metallobiochemistry. Part B Metallothionein and Related Molecules*, ed. J. F. Riordan and B. L. Vallee, Academic Press, Inc., San Diego, 1991, vol. 205, pp. 8–10.
2 M. Margoshes and B. L. Vallee, *J. Am. Chem. Soc.*, 1957, **79**, 4813–4814.
3 J. H. R. Kagi and B. L. Vallee, *J. Biol. Chem.*, 1960, **235**, 3460–3465.
4 J. H. R. Kagi, in *Metallothionein III: Biological Roles and Medical Implications*, ed. K. T. Suzuki, N. Imura and M. Kimura, Birkhauser-Verlag, Berlin, 1993, pp. 29–55.
5 A. H. Robbins, D. E. McRee, M. Williamson, S. A. Collett, N. H. Xuong, W. F. Furey, B. C. Wang and C. D. Stout, *J. Mol. Biol.*, 1991, **221**, 1269–1293.
6 P.-A. Binz and J. H. R. Kagi, in *Metallothionein IV*, ed. C. D. Klaassen, Birkhauser, Berlin, 1999, pp. 7–13.
7 K. K. Kramer, J. T. Zoelle and C. D. Klaassen, *Toxicol. Appl. Pharmacol.*, 1996, **141**, 1–7.
8 K. K. Kramer, J. Liu, S. Choudhuri and C. D. Klaassen, *Toxicol. Appl. Pharmacol.*, 1996, **136**, 94–100.
9 Y. Uchida, K. Takio, K. Titani, Y. Ihara and M. Tomonaga, *Neuron*, 1991, **7**, 337–347.
10 C. J. Quaife, S. D. Findley, J. C. Erickson, G. J. Froelick, E. J. Kelly, B. P. Zambrowicz and R. D. Palmiter, *Biochemistry*, 1994, **33**, 7250–7259.
11 C. J. Quaife, E. J. Kelly, B. A. Masters, R. L. Brinster and R. D. Palmiter, *Toxicol. Appl. Pharmacol.*, 1998, **148**, 148–157.
12 Y. Li and W. Maret, *J. Anal. At. Spectrom.*, 2008, **23**, 1055–1062.
13 L. Ryden and H. F. Deutsch, *J. Biol. Chem.*, 1978, **253**, 519–524.
14 H.-J. Hartmann and U. Weser, *Biochim. Biophys. Acta*, 1977, **491**, 211–222.
15 R. W. Briggs and I. M. Armitage, *J. Biol. Chem.*, 1982, **257**, 1259–1262.
16 J. A. Szymanska, A. J. Zelazowski and M. J. Stillman, *Biochem. Biophys. Res. Commun.*, 1983, **115**, 167–173.
17 M. J. Stillman, Z. Gasyna and A. J. Zelazowski, *FEBS Lett.*, 1989, **257**, 283–286.
18 B. Dolderer, H.-J. Hartmann and U. Weser, in *Metal Ions in Life Sciences*, ed. A. Sigel, H. Sigel and R. K. O. Sigel, The Royal Society of Chemistry, Cambridge, 2009, vol. 5, pp. 83–105.
19 C. E. Outten and T. V. O'Halloran, *Science*, 2001, **292**, 2488–2492.
20 T. D. Rae, P. J. Schmidt, R. A. Pufahl, V. C. Culotta and T. V. O'Halloran, *Science*, 1999, **284**, 805–808.
21 W. Feng, J. Cai, W. M. Pierce, R. B. Franklin, W. Maret, F. W. Benz and Y. J. Kang, *Biochem. Biophys. Res. Commun.*, 2005, **332**, 853–858.
22 A. Z. Mason, N. Perico, R. Moeller, K. Thrippleton, T. Potter and D. Lloyd, *Mar. Environ. Res.*, 2004, **58**, 371–375.
23 W. Maret, K. S. Larsen and B. L. Vallee, *Proc. Natl. Acad. Sci. U. S. A.*, 1997, **94**, 2233–2237.
24 J. Zeng, R. Heuchel, W. Schaffner and J. H. R. Kagi, *FEBS Lett.*, 1991, **279**, 310–312.
25 D. J. Ecker, T. R. Butt, E. J. Sternberg, M. P. Neeper, C. Debouck, J. A. Gorman and S. T. Crooke, *J. Biol. Chem.*, 1986, **261**, 16895–16900.
26 T. R. Butt, E. J. Sternberg, J. A. Gorman, P. Clark, D. Hamer, M. Rosenberg and S. T. Crooke, *Proc. Natl. Acad. Sci. U. S. A.*, 1984, **81**, 3332–3336.
27 F. Bonneton, L. Theodore, P. Silar, G. Maroni and M. Wegnez, *FEBS Lett.*, 1996, **380**, 33–38.
28 G. W. Stuart, P. F. Searle, H. Y. Chen, R. L. Brinster and R. D. Palmiter, *Proc. Natl. Acad. Sci. U. S. A.*, 1984, **81**, 7318–7322.
29 A. D. Carter, B. K. Felber, M. Walling, M.-F. Jubier, C. J. Schmidt and D. H. Hamer, *Proc. Natl. Acad. Sci. U. S. A.*, 1984, **81**, 7392–7396.
30 G. K. Andrews, *Biochem. Pharmacol.*, 2000, **59**, 95–104.
31 G. W. Stuart, P. F. Searle and R. D. Palmiter, *Nature*, 1985, **317**, 828–831.
32 X. Chen, M. Chu and D. P. Giedroc, *Biochemistry*, 1999, **38**, 12915–12925.
33 D. P. Giedroc, X. Chen, M. A. Pennella and A. C. LiWang, *J. Biol. Chem.*, 2001, **276**, 42322–42332.
34 B. Zhang, O. Georgiev, M. Hagmann, C. Gunes, M. Cramer, P. Faller, M. Vasak and W. Schaffner, *Mol. Cell. Biol.*, 2003, **23**, 8471–8485.
35 B. L. Vallee, in *Experientia Supplementum: Metallothionein*, ed. J. H. R. Kagi and M. Nordberg, Birkhauser Verlag, Boston, 1979, vol. 34, pp. 19–40.
36 P. Pulido, J. H. R. Kagi and B. L. Vallee, *Biochemistry*, 1966, **5**, 1768–1777.
37 K. B. Nielson, C. L. Atkin and D. R. Winge, *J. Biol. Chem.*, 1985, **260**, 5342–5350.
38 M. Good and M. Vasak, *Biochemistry*, 1986, **25**, 8353–8356.
39 M. M. Morelock, T. A. Cormier and G. L. Tolman, *Inorg. Chem.*, 1988, **27**, 3137–3140.
40 T. T. Ngu, S. Krecisz and M. J. Stillman, *Biochem. Biophys. Res. Commun.*, 2010, **396**, 206–212.

41 M. Vasak, *J. Am. Chem. Soc.*, 1980, **102**, 3953–3955.
42 L. Cai, X.-K. Li, Y. Song and M. G. Cherian, *Curr. Med. Chem.*, 2005, **12**, 2753–2763.
43 E. J. Kelly, C. J. Quaife, G. J. Froelick and R. D. Palmiter, *J. Nutr.*, 1996, **126**, 1782–1790.
44 H. Kodama and C. Fujisawa, *Metallomics*, 2009, **1**, 42–52.
45 M. Suzuki-Kurasaki, M. Okabe and M. Kurasaki, *J. Histochem. Cytochem.*, 1997, **45**, 1493–1501.
46 E. J. Kelly and R. D. Palmiter, *Nat. Genet.*, 1996, **13**, 219–222.
47 N. O. Nartey, J. V. Frei and M. G. Cherian, *Lab. Invest.*, 1987, **57**, 397–401.
48 N. Chiaverini and M. DeLey, *Free Radical Res.*, 2010, **44**, 605–613.
49 Y. J. Kang, *Exp. Biol. Med.*, 2006, **231**, 1459–1467.
50 H. M. Chan, L.-F. Zhu, R. Zhong, D. Grant, R. A. Goyer and M. G. Cherian, *Toxicol. Appl. Pharmacol.*, 1993, **123**, 89–96.
51 J. Liu, Y. Liu, S. S. Habeebu and C. D. Klaassen, *Toxicol. Sci.*, 1998, **46**, 197–203.
52 C. D. Klaassen, J. Liu and B. A. Diwan, *Toxicol. Appl. Pharmacol.*, 2009, **238**, 215–220.
53 Y. Suwazono, T. Kido, H. Nakagawa, M. Nishijo, R. Honda, E. Kobayashi, M. Dochi and K. Nogawa, *Biomarkers*, 2009, **14**, 77–81.
54 B. A. Masters, E. J. Kelly, C. J. Quaife, R. L. Brinster and R. D. Palmiter, *Proc. Natl. Acad. Sci. U. S. A.*, 1994, **91**, 584–588.
55 J. D. Park, Y. Liu and C. D. Klaassen, *Toxicology*, 2001, **163**, 93–100.
56 A. K. West, J. Hidalgo, D. Eddins, E. D. Levin and M. Aschner, *NeuroToxicology*, 2008, **29**, 489–503.
57 D. E. K. Sutherland and M. J. Stillman, *Biochem. Biophys. Res. Commun.*, 2008, **372**, 840–844.
58 K. E. Rigby-Duncan and M. J. Stillman, *FEBS J.*, 2007, **274**, 2253–2261.
59 P. Palumaa, E. Eriste, O. Njunkova, L. Pokras, H. Jornvall and R. Sillard, *Biochemistry*, 2002, **41**, 6158–6163.
60 Y. J. Kang, G. Li and J. T. Saari, *Am. J. Physiol.*, 1999, **276**, H993–H997.
61 Y. J. Kang, Y. Li, X. Sun and X. Sun, *Am. J. Pathol.*, 2003, **163**, 1579–1586.
62 C. M. St.Croix, K. J. Wasserloos, K. E. Dineley, I. J. Reynolds, E. S. Levitan and B. R. Pitt, *Am. J. Physiol. Lung Cell Mol. Physiol.*, 2002, **282**, L185–L192.
63 K. Zangger, G. Oz, E. Haslinger, O. Kunert and I. M. Armitage, *FASEB J.*, 2001, **15**, 1303–1305.
64 L. Khatai, W. Goessler, H. Lorencova and K. Zangger, *Eur. J. Biochem.*, 2004, **271**, 2408–2416.
65 H. Wang, H. Li, B. Cai, Z.-X. Huang and H. Sun, *J. Biol. Inorg. Chem.*, 2008, **13**, 411–419.
66 W. G. Elgohary, S. Sidhu, S. O. Krezoski, D. H. Petering and R. W. Byrnes, *Chem.-Biol. Interact.*, 1998, **115**, 85–107.
67 A. R. Quesada, R. W. Byrnes, S. O. Krezoski and D. H. Petering, *Arch. Biochem. Biophys.*, 1996, **334**, 241–250.
68 L. Cai, J. Koropatnick and M. G. Cherian, *Chem.-Biol. Interact.*, 1995, **96**, 143–155.
69 W. Maret, *Exp. Gerontol.*, 2008, **43**, 363–369.
70 V. Calderone, B. Dolderer, H.-J. Hartmann, H. Echner, C. Luchinat, C. DelBianco, S. Mangani and U. Weser, *Proc. Natl. Acad. Sci. U. S. A.*, 2005, **102**, 51–56.
71 A. Arseniev, P. Schultze, E. Worgotter, W. Braun, G. Wagner, M. Vasak, J. H. R. Kagi and K. Wuthrich, *J. Mol. Biol.*, 1988, **201**, 637–657.
72 B. A. Messerle, A. Schaffer, M. Vasak, J. H. R. Kagi and K. Wuthrich, *J. Mol. Biol.*, 1990, **214**, 765–779.
73 P. Schultze, E. Worgotter, W. Braun, G. Wagner, M. Vasak, J. H. R. Kagi and K. Wuthrich, *J. Mol. Biol.*, 1988, **203**, 251–268.
74 K. Zangger, G. Oz, J. D. Otvos and I. M. Armitage, *Protein Sci.*, 1999, **8**, 2630–2638.
75 W. Braun, M. Vasak, A. H. Robbins, C. D. Stout, G. Wagner, J. H. R. Kagi and K. Wuthrich, *Proc. Natl. Acad. Sci. U. S. A.*, 1992, **89**, 10124–10128.
76 B. A. Messerle, A. Schaffer, M. Vasak, J. H. R. Kagi and K. Wuthrich, *J. Mol. Biol.*, 1992, **225**, 433–443.
77 A. Presta, A. R. Green, A. Zelazowski and M. J. Stillman, *Eur. J. Biochem.*, 1995, **227**, 226–240.
78 L. T. Jensen, J. M. Peltier and D. R. Winge, *J. Biol. Inorg. Chem.*, 1998, **3**, 627–631.
79 G. Meloni, P. Faller and M. Vasak, *J. Biol. Chem.*, 2007, **282**, 16068–16078.
80 M. J. Stillman, in *Metallothioneins: Synthesis, Structure and Properties of Metallothioneins, Phytochelatines and Metal–Thiolate Complexes*, ed. M. J. Stillman, C. F. Shaw-III and K. T. Suzuki, VCH Publishers, New York, 1992, pp. 55–120.
81 H. Rupp and U. Weser, *Biochim. Biophys. Acta*, 1978, **533**, 209–226.
82 D. E. K. Sutherland, M. J. Willans and M. J. Stillman, *Biochemistry*, 2010, **49**, 3593–3601.
83 K. E. Rigby-Duncan, C. W. Kirby and M. J. Stillman, *FEBS J.*, 2008, **275**, 2227–2239.
84 A. R. Green, A. Presta, Z. Gasyna and M. J. Stillman, *Inorg. Chem.*, 1994, **33**, 4159–4168.
85 A. Torreggiani and A. Tinti, *Metallomics*, 2010, **2**, 246–260.
86 T. T. Ngu, A. Easton and M. J. Stillman, *J. Am. Chem. Soc.*, 2008, **130**, 17016–17028.
87 A. Krezel and W. Maret, *J. Am. Chem. Soc.*, 2007, **129**, 10911–10921.
88 S. R. Sturzenbaum, O. Georgiev, A. J. Morgan and P. Kille, *Environ. Sci. Technol.*, 2004, **38**, 6283–6289.
89 S. R. Sturzenbaum, P. Kille and A. J. Morgan, *FEBS Lett.*, 1998, **431**, 437–442.
90 S. R. Sturzenbaum, C. Winters, M. Galay, A. J. Morgan and P. Kille, *J. Biol. Chem.*, 2001, **276**, 34013–34018.
91 T. T. Ngu, S. R. Sturzenbaum and M. J. Stillman, *Biochem. Biophys. Res. Commun.*, 2006, **351**, 229–233.
92 C. A. Morris, B. Nicolaus, V. Sampson, J. L. Harwood and P. Kille, *Biochem. J.*, 1999, **338**, 553–560.
93 M. E. Merrifield, J. Chaseley, P. Kille and M. J. Stillman, *Chem. Res. Toxicol.*, 2006, **19**, 365–375.
94 O. I. Leszczyszyn, C. D. Evans, S. E. Keiper, G. Z. L. Warren and C. A. Blindauer, *Inorg. Chim. Acta*, 2007, **360**, 3–13.
95 C. A. Blindauer, M. T. Razi, D. J. Campopiano and P. J. Sadler, *J. Biol. Inorg. Chem.*, 2007, **12**, 393–405.
96 E. A. Peroza, R. Schmucki, P. Guntert, E. Freisinger and O. Zerbe, *J. Mol. Biol.*, 2009, **387**, 207–218.
97 G. Meloni, T. Polanski, O. Braun and M. Vasak, *Biochemistry*, 2009, **48**, 5700–5707.
98 I. Bertini, C. Luchinat, L. Messori and M. Vasak, *J. Am. Chem. Soc.*, 1989, **111**, 7296–7300.
99 M. Vasak and J. H. R. Kagi, *Proc. Natl. Acad. Sci. U. S. A.*, 1981, **78**, 6709–6713.
100 A. Krezel and W. Maret, *Biochem. J.*, 2007, **402**, 551–558.
101 U. Rana, R. Kothinti, J. Meeusen, N. M. Tabatabai, S. Krezoski and D. H. Petering, *J. Inorg. Biochem.*, 2008, **102**, 489–499.
102 E. Mocchegiani, R. Giacconi, E. Muti, C. Cipriano, L. Costarelli, S. Tesei, N. Gasparini and M. Malavolta, *Immun. Ageing*, 2007, **4**, 7, DOI: 10.1186/1742-4933-4-7.
103 R. Giacconi, A. R. Bonfigli, R. Testa, C. Sirolla, C. Cipriano, M. Marra, E. Muti, M. Malavolta, L. Costarelli, F. Piacenza, S. Tesei and E. Mocchegiani, *Mol. Genet. Metab.*, 2008, **94**, 98–104.
104 W. Maret, *Mol. Genet. Metab.*, 2008, **94**, 1–3.
105 J. Ejnik, J. Robinson, J. Zhu, H. Forsterling and C. F. Shaw-III, *J. Inorg. Biochem.*, 2002, **88**, 144–152.
106 T. T. Ngu, J. A. Lee, T. B. J. Pinter and M. J. Stillman, *J. Inorg. Biochem.*, 2010, **104**, 232–244.
107 T. T. Ngu and M. J. Stillman, *J. Am. Chem. Soc.*, 2006, **128**, 12473–12483.
108 T. T. Ngu, J. A. Lee, M. K. Rushton and M. J. Stillman, *Biochemistry*, 2009, **48**, 8806–8816.
109 T. T. Ngu, M. D. M. Dryden and M. J. Stillman, *Biochem. Biophys. Res. Commun.*, 2010, **401**, 69–74.
110 K. Balamurugan and W. Schaffner, in *Metal Ions in Life Sciences*, ed. A. Sigel, H. Sigel and R. K. O. Sigel, The Royal Society of Chemistry, Cambridge, 2009, vol. 5, pp. 31–49.
111 C. Giaginis, E. Gatzidou and S. Theocharis, *Toxicol. Appl. Pharmacol.*, 2006, **213**, 282–290.
112 J. Liu, W. Qu and M. B. Kadiiska, *Toxicol. Appl. Pharmacol.*, 2009, **238**, 209–214.
113 L. Jarup and A. Akesson, *Toxicol. Appl. Pharmacol.*, 2009, **238**, 201–208.

114 J. Kobayashi, in *Toxicity of Heavy Metals in the Environment*, ed. F. W. Oehme, Marcel Dekker, Inc., New York, 1978, vol. 1, pp. 199–260.
115 Y. Boulanger, I. M. Armitage, K.-A. Miklossy and D. R. Winge, *J. Biol. Chem.*, 1982, **257**, 13717–13719.
116 A. Galdes, M. Vasak, H. A. O. Hill and J. H. R. Kagi, *FEBS Lett.*, 1978, **92**, 17–21.
117 H. Rupp, W. Voelter and U. Weser, *FEBS Lett.*, 1974, **40**, 176–179.
118 M. Vasak, A. Galdes, H. A. O. Hill, J. H. R. Kagi, I. Bremner and B. W. Young, *Biochemistry*, 1980, **19**, 416–425.
119 J. D. Otvos and I. M. Armitage, *Proc. Natl. Acad. Sci. U. S. A.*, 1980, **77**, 7094–7098.
120 J. D. Otvos and I. M. Armitage, *J. Am. Chem. Soc.*, 1979, **101**, 7734–7736.
121 P. J. Sadler, A. Bakka and P. J. Beynon, *FEBS Lett.*, 1978, **94**, 315–318.
122 C. T. Hunt, Y. Boulanger, S. W. Fesik and I. M. Armitage, *Environ. Health Perspect.*, 1984, **54**, 135–145.
123 C. A. Blindauer, M. D. Harrison, J. A. Parkinson, A. K. Robinson, J. S. Cavet, N. J. Robinson and P. J. Sadler, *Proc. Natl. Acad. Sci. U. S. A.*, 2001, **98**, 9593–9598.
124 J. R. Prohaska, *Am. J. Clin. Nutr.*, 2008, **88**, 826S–829S.
125 G. Meloni, V. Sonois, T. Delaine, L. Guilloreau, A. Gillet, J. Teissie, P. Faller and M. Vasak, *Nat. Chem. Biol.*, 2008, **4**, 366–372.
126 M. Beltramini and K. Lerch, *FEBS Lett.*, 1981, **127**, 201–203.
127 M. T. Salgado and M. J. Stillman, *Biochem. Biophys. Res. Commun.*, 2004, **318**, 73–80.
128 Y.-J. Li and U. Weser, *Inorg. Chem.*, 1992, **31**, 5526–5533.
129 K. B. Nielson and D. R. Winge, *J. Biol. Chem.*, 1984, **259**, 4941–4946.
130 J. Ejnik, C. F. Shaw-III and D. H. Petering, *Inorg. Chem.*, 2010, **49**, 6525–6534.
131 T. Gan, A. Munoz, C. F. Shaw-III and D. H. Petering, *J. Biol. Chem.*, 1995, **270**, 5339–5345.
132 M. J. Stillman, D. Thomas, C. Trevithick, X. Guo and M. Siu, *J. Inorg. Biochem.*, 2000, **79**, 11–19.
133 M. T. Salgado, K. L. Bacher and M. J. Stillman, *J. Biol. Inorg. Chem.*, 2007, **12**, 294–312.
134 M. Yoshida, C. Watanabe, K. Horie, M. Satoh, M. Sawada and A. Shimada, *Toxicol. Lett.*, 2005, **155**, 361–368.
135 M. Yoshida, C. Watanabe, M. Satoh, A. Yasutake, M. Sawada, Y. Ohtsuka, Y. Akama and C. Tohyama, *Toxicol. Sci.*, 2004, **80**, 69–73.
136 M. Yoshida, C. Watanabe, M. Kishimoto, A. Yasutake, M. Satoh, M. Sawada and Y. Akama, *Toxicol. Lett.*, 2006, **161**, 210–218.
137 M. Satoh, N. Nishimura, Y. Kanayama, A. Naganuma, T. Suzuki and C. Tohyama, *J. Pharmacol. Exp. Ther.*, 1997, **283**, 1529–1533.
138 J. P. K. Rooney, *Toxicology*, 2007, **234**, 145–156.
139 M. Aschner, D. R. Conklin, C. Ping-Yao, J. W. Allen and K. H. Tan, *Brain Res.*, 1998, **813**, 254–261.
140 L. Rising, D. Vitarella, H. K. Kimelberg and M. Aschner, *J. Neurochem.*, 1995, **65**, 1562–1568.
141 W. Lu and M. J. Stillman, *J. Am. Chem. Soc.*, 1993, **115**, 3291–3299.
142 W. Lu, A. J. Zelazowski and M. J. Stillman, *Inorg. Chem.*, 1993, **32**, 919–926.
143 A. Leiva-Presa, M. Capdevila and P. Gonzalez-Duarte, *Eur. J. Biochem.*, 2004, **271**, 4872–4880.
144 W. Cai and M. J. Stillman, *J. Am. Chem. Soc.*, 1988, **110**, 7872–7873.
145 W. Lu, M. Kasrai, G. M. Bancroft, M. J. Stillman and K. H. Tan, *Inorg. Chem.*, 1990, **29**, 2561–2563.
146 D. T. Jiang, S. M. Heald, T. K. Sham and M. J. Stillman, *J. Am. Chem. Soc.*, 1994, **116**, 11004–11013.
147 A. M. Scheuhammer and M. G. Cherian, *Toxicol. Appl. Pharmacol.*, 1986, **82**, 417–425.
148 E. A. Peroza, A. Al-Kaabi, W. Meyer-Klaucke, G. Wellenreuther and E. Freisinger, *J. Inorg. Biochem.*, 2009, **103**, 342–353.
149 N. Felitsyn, M. Peschke and P. Kebarle, *Int. J. Mass Spectrom.*, 2002, **219**, 39–62.
150 P. Kebarle and U. H. Verkerk, *Mass Spectrom. Rev.*, 2009, **28**, 898–917.
151 N. Romero-Isart, L. T. Jensen, O. Zerbe, D. R. Winge and M. Vasak, *J. Biol. Chem.*, 2002, **277**, 37023–37028.
152 A. K. Sewell, L. T. Jensen, J. C. Erickson, R. D. Palmiter and D. R. Winge, *Biochemistry*, 1995, **34**, 4740–4747.
153 J. Chan, Z. Huang, I. Watt, P. Kille and M. J. Stillman, *Can. J. Chem.*, 2007, **85**, 898–912.